



Synthesis and biological evaluation of 2-fluoro and 3-trifluoromethyl-phenyl-piperazinylalkyl derivatives of 1*H*-imidazo[2,1-*f*]purine-2,4(3*H*,8*H*)-dione as potential antidepressant agents

Agnieszka Zagórska, Adam Bucki, Marcin Kołaczkowski, Agata Siwek, Monika Głuch-Lutwin, Gabriela Starowicz, Grzegorz Kazek, Anna Partyka, Anna Wesołowska, Karolina Słoczyńska, Elżbieta Pękala & Maciej Pawłowski

To cite this article: Agnieszka Zagórska, Adam Bucki, Marcin Kołaczkowski, Agata Siwek, Monika Głuch-Lutwin, Gabriela Starowicz, Grzegorz Kazek, Anna Partyka, Anna Wesołowska, Karolina Słoczyńska, Elżbieta Pękala & Maciej Pawłowski (2016) Synthesis and biological evaluation of 2-fluoro and 3-trifluoromethyl-phenyl-piperazinylalkyl derivatives of 1*H*-imidazo[2,1-*f*]purine-2,4(3*H*,8*H*)-dione as potential antidepressant agents, *Journal of Enzyme Inhibition and Medicinal Chemistry*, 31:sup3, 10-24, DOI: [10.1080/14756366.2016.1198902](https://doi.org/10.1080/14756366.2016.1198902)

To link to this article: <https://doi.org/10.1080/14756366.2016.1198902>

 [View supplementary material](#)

 [Published online: 29 Jun 2016.](#)

 [Submit your article to this journal](#)

 [Article views: 1766](#)

 [View related articles](#)

 [View Crossmark data](#)

 [Citing articles: 5 View citing articles](#)

RESEARCH ARTICLE

Synthesis and biological evaluation of 2-fluoro and 3-trifluoromethyl-phenyl-piperazinylalkyl derivatives of 1*H*-imidazo[2,1-*f*]purine-2,4(3*H*,8*H*)-dione as potential antidepressant agents

Agnieszka Zagórska¹, Adam Bucki¹, Marcin Kołaczkowski¹, Agata Siwek², Monika Głuch-Lutwin³, Gabriela Starowicz³, Grzegorz Kazek³, Anna Partyka⁴, Anna Wesołowska⁴, Karolina Słoczyńska⁵, Elżbieta Pękała⁵, and Maciej Pawłowski¹

¹Department of Medicinal Chemistry, ²Department of Pharmacobiology, ³Department of Pharmacodynamics, ⁴Department of Clinical Pharmacy, and ⁵Department of Pharmaceutical Biochemistry, Jagiellonian University Medical College, Kraków, Poland

Abstract

A series of 2-fluoro and 3-trifluoromethylphenylpiperazinylalkyl derivatives of 1*H*-imidazo[2,1-*f*]purine-2,4(3*H*,8*H*)-dione (**4–21**) were synthesized and evaluated for their serotonin (5-HT_{1A}/5-HT₇) receptor affinity and phosphodiesterase (PDE4B and PDE10A) inhibitor activity. The study enabled the identification of potent 5-HT_{1A}, 5-HT₇ and mixed 5-HT_{1A}/5-HT₇ receptor ligands with weak inhibitory potencies for PDE4B and PDE10A. The tests have been completed with the determination of lipophilicity and metabolic stability using micellar electrokinetic chromatography (MEKC) system and human liver microsomes (HLM) model. In preliminary pharmacological *in vivo* studies, selected compound 8-(5-(4-(2-fluorophenyl)piperazin-1-yl)pentyl)-1,3,7-trimethyl-1*H*-imidazo[2,1-*f*]purine-2,4(3*H*,8*H*)-dione (**9**) behaved as a potential antidepressant in forced swim test (FST) in mice. Moreover, potency of anti-anxiety effects evoked by **9** (2.5 mg/kg) is greater than that of the reference anxiolytic drug, diazepam. Molecular modeling revealed that fluorinated arylpiperazinylalkyl derivatives of 1*H*-imidazo[2,1-*f*]purine-2,4(3*H*,8*H*)-dione have major significance for the provision of lead compounds for antidepressant and/or anxiolytic application.

Introduction

Over the past decade, we have witnessed unparalleled advances in our understanding of the basic biological processes that contribute to many human disorders, although a detailed understanding of the etiology of complex psychiatric disorders remains elusive. Psychiatric diseases are chronic and recurrent and have a complex etiology. Human genomics and biological studies have revealed an unprecedented number of promising molecular targets for neuropsychiatric disorders, including G-protein-coupled receptors and transporters, intracellular and synaptic proteins and microRNAs. Serotonin (5-HT) is one of the most attractive targets for medicinal chemists and the discovery of ligands with affinity for the family of 5-HT receptors (5-HTRs) is an area of intense research, because of the potential to find new therapeutic drugs, due to their involvement in numerous physiological and pathophysiological processes. Among the 14 5-HTRs identified, the 5-HT_{1A} and 5-HT₇ subtypes are the best studied due to effects of their full or partial agonists or antagonists on anxiety,

Keywords

Depression, long-chain arylpiperazines, PDE, phosphodiesterase inhibitors, serotonin

History

Received 7 December 2015

Revised 27 May 2016

Accepted 1 June 2016

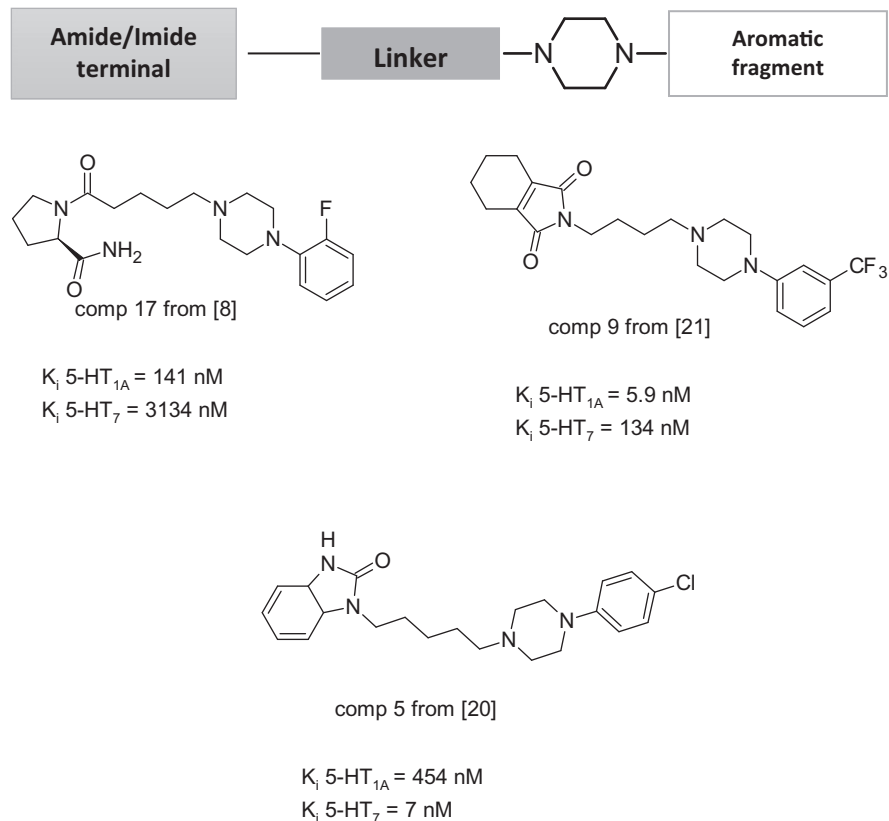
Published online 23 June 2016

depression and schizophrenia^{1–6}. A very important class of 5-HT receptors ligands are derivatives of 1,4-disubstituted arylpiperazine (Figure 1). Such arylpiperazine derivative with long-chain substituents incorporated on the basic nitrogen of the phenylpiperazine ring – long-chain arylpiperazines (LCAPs) – are commonly studied classes of bioactive compounds^{7–24}. Despite the enormous progress in central nervous system (CNS) drug discovery, particularly in the areas of mood disorders and schizophrenia, new drugs are still being sought. The main reasons behind the search for novel therapeutics are poor patient compliance, delayed onset of action and side effects, including emesis, sexual dysfunction, weight gain, diabetes mellitus or endocrinopathies. Roth et al. proposed that, for mood disorders and schizophrenia, attempting to develop more effective treatments by intentionally designing nonselective drugs that interact with several molecular targets would lead to new and more effective medications (“magic shotguns”)²⁵.

Cyclic nucleotide phosphodiesterases (PDEs) are a superfamily of enzymes that are involved in the regulation of the intracellular second messenger’s cyclic AMP (cAMP) and cyclic GMP (cGMP) by controlling their rates of hydrolysis. There are 11 different PDE families and each family typically has multiple isoforms and splice variants. The PDEs differ in their structures, distribution, modes of regulation and sensitivity to inhibitors.

Address for correspondence: A. Zagórska, Department of Medicinal Chemistry, Jagiellonian University Medical College, 9 Medyczna Street, 30-688 Kraków, Poland. Tel: +48 12 62 05 450. Fax: +48 12 62 05 458. E-mail: agnieszka.zagorska@uj.edu.pl

Figure 1. General structure of long-chain arylpiperazine (LCAPs) and their representatives of 5-HT_{1A} and 5-HT₇ receptor ligands.



Since PDEs have been shown to play distinct roles in the processes of emotion and related learning and memory processes, selective PDE inhibitors, by preventing the breakdown of cAMP and/or cGMP, modulate mood and related cognitive activity. It is becoming increasingly clear that PDE inhibitors have therapeutic potential for the treatment of neuropsychiatric disorders involving disturbances of mood, emotion and cognition²⁶. Moreover, PDE4 and PDE10 due to their presence in areas of the brain associated with the site of action of psychotropic drugs and their inhibitors have potential therapeutic relevance. In animal models, elevated intracellular cAMP level achieved by PDE inhibition have been shown to possess antidepressant-like effect. Moreover, antipsychotic effects can be reproduced by inhibition of the enzymes that degrade cAMP. Maxwell et al. used amphetamine-induced abnormalities in auditory event-related potentials to study the antipsychotic potential of nonreceptor based compounds such as rolipram^{27,28}. The therapeutic potentials of PDE inhibitors have been explored in many areas; for instance, PDE4 inhibitors have been evaluated for the treatment of cognitive disorders, depression, and anxiety and PDE10 inhibitors for the treatment of schizophrenia and Huntington's disease. Naturally occurring methylxanthines (theophylline, caffeine) were the first inhibitors of PDE to be discovered. To improve the potency and specificity for the inhibition of various PDEs, thousands of compounds with related structures have been synthesized. Today, selective inhibitors of PDE4 and PDE10 show a large of chemical diversity (Figure 2).

For years, our attention has been focused on the development of LCAPs with the complex terminal part based on a purine moiety. Annulated derivatives of theophylline with an LCAP moiety demonstrate high affinity toward serotonin 5-HT_{1A} and moderate affinity to 5-HT_{2A} and 5-HT₇ and the dopaminergic D₂ receptor site. Preclinical results indicate that monosubstituted derivatives of LCAPs with an imidazo[2,1-*f*]purine-2,4-dione as the terminal part act as antipsychotics with additional

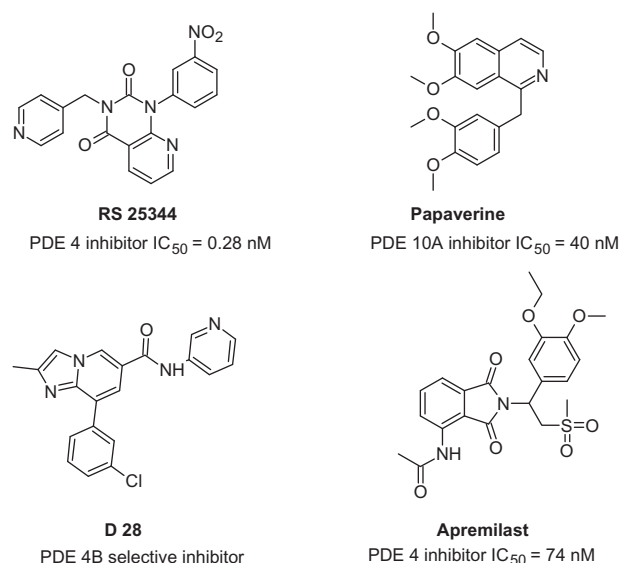


Figure 2. Chemical structures and inhibitor activity (IC₅₀) of inhibitors of PDE4 and PDE10.

antidepressant and anxiolytic properties^{29–32}. In view of this and our earlier chemical and pharmacological investigation, in the current study, we designed and synthesized a new series of 2-fluoro and 3-trifluoromethylphenylpiperazinyalkyl derivatives of 1*H*-imidazo[2,1-*f*]purine-2,4(3*H*,8*H*)-diones. The special properties of fluorine, such as its high electronegativity, small size and very low polarizability, impart a variety of properties important in medicinal chemistry. Fluoro or trifluoromethyl substitutions will generally have enhanced binding interactions, metabolic stability, changes in physicochemical properties and selective relationships toward of targeted molecules. Fluorinated

drugs constitute the first (spiperone, haloperidol, droperidol) and second (risperidone, sertindole, paliperidone, iloperidone) generation of antipsychotic drugs and antidepressants (fluvoxamine, paroxetine, citalopram) from the selective serotonin reuptake inhibitors (SSRIs) group with extremely famous fluoxetine (Prozac®). Herein, we examined the effect of fluorine substitution on receptor affinity, selectivity, intrinsic activity for 5-HT_{1A} and 5-HT₇ receptor, and lipophilicity. Moreover, studies focused on the effect of the presence of annelated imidazole moiety at the 7, 8 position of purine system on PDE4B/PDE10A inhibition and metabolic stability. Finally, structure–activity relationships were analyzed and explained by molecular modeling.

Experimental protocols

Chemistry

Organic solvents (from Sigma-Aldrich and Chempur) were of reagent grade and were used without purification. All other reagents were from Sigma-Aldrich and Alfa Aesar. Thin-layer chromatography (TLC) was performed on Merck silica gel 60 F254 aluminum sheets (Merck, Darmstadt, Germany). Spots were detected by their absorption under UV light ($\lambda = 254$ nm). Analytical high-performance liquid chromatography (HPLC) was run on an Alliance Waters 2695 Separations Module equipped with a Chromolith SpeedROD RP 18.5 μ m column (4.6 \times 50 mm). Standard conditions were eluent system A (water/0.1% TFA), system B (acetonitrile/0.1% TFA). A flow rate of 5 mL/min and a gradient of (0–100)% B over 3 min were used. Detection was performed on a photodiode array (PDA) detector. Retention times (t_R) are given in minutes. Nuclear magnetic resonance (NMR) spectra were measured in CDCl₃ on a Varian Mercury-VX 300 spectrometer operating at 300.08 MHz (¹H), 282 MHz (¹⁹F) and 75.46 MHz (¹³C). Sample concentrations were in the range from 10 mg/1 mL (¹H and ¹⁹F) to 50 mg/mL for ¹³C, all spectra were acquired at 26 °C. The *J* values are in Hertz (Hz), and splitting patterns are designated as follows: s (singlet), d (doublet), t (triplet), m (multiplet). Mass spectrometry analyses: Samples were prepared in acetonitrile/water (10/90 v/v) mixture. The LC/MS system consisted of a Waters Acquity UPLC, coupled to Waters TQD mass spectrometer (electrospray ionization mode ESI-tandem quadrupole). All the analyses were carried out using an Acquity UPLC BEH C₁₈, 50 \times 2.1 mm reversed-phase column. A flow rate of 0.3 mL/min and a gradient of (5–5)% B over 5 min was used. Eluent A: water/0.1% HCO₂H; eluent B: acetonitrile/0.1% HCO₂H. Nitrogen was used for both nebulizing and drying gas. LC/MS data were obtained by scanning the first quadrupole in 0.5 s in a mass range from 100 to 700 *m/z*; eight scans were summed up to produce the final spectrum. Elemental analyses were found within $\pm 0.4\%$ of the theoretical values. Melting points (mp) were determined with a Büchi apparatus and are uncorrected. Column chromatography separations were carried out on column with Merck Kieselgel 60 (Darmstadt, Germany).

General procedure for the synthesis of phthalimide derivatives (VI–XI)

A mixture of 10 mmol of 1-(2-fluorophenyl)- or 1-(3-trifluoromethylphenyl)piperazine (I–II) and 10 mmol of appropriate 2-(bromoalkyl)-1*H*-isoindoline-1,3(2*H*)-dione (III–V), 30 mmol of potassium carbonate, catalytic amount of potassium iodide and 20 mL of acetonitrile was stirred at 82 °C temperature for 48 h. The reaction mixture evaporated under reduced pressure to obtain a residue, which was purified by column chromatography using dichloromethane/methanol (9/1) as an eluent.

General procedure for the deprotection of the phthalimide group (XII–XVI)

A mixture of 1.2 mmol of appropriate compound VI–XI and 65% hydrazine monohydrate aqueous solution (15 mmol) in 99.8% ethanol were refluxed for 1 h. The reaction mixtures were cooled down and treated with an additional amount of 99.8% ethanol and concentrated HCl (1.3 mL). Then, the reaction mixtures were refluxed for 4 h and left overnight in a refrigerator. The precipitates were filtered off, and the solvents were evaporated. The residues were treated with *n*-hexane (20 mL) and NH₃ (aqueous, 15 mL). The solutions were extracted with methylene chloride (3 \times 15 mL), the combined extracts were dried over anhydrous Na₂SO₄, and the solvents were evaporated to give a products that were used without further purification (yield: 70–80%).

General procedure for 7-ketonyl derivatives of 8-bromo-1,3-dimethyl-3,7-dihydro-1*H*-purine-2,6-dione (1–3)

2-(8-Bromo-1,3-dimethyl-2,6-dioxo-1,2,3,6-tetrahydro-7*H*-purin-7-yl)acetaldehyde (1) was obtained according to the previously described procedure²⁹. 8-Bromo-1,3-dimethyl-7-(2-oxopropyl)-3,7-dihydro-1*H*-purine-2,6-dione (2) and 8-bromo-1,3-dimethyl-7-(2-oxo-2-phenylethyl)-3,7-dihydro-1*H*-purine-2,6-dione (3) were obtained as described below. 8-Bromo-1,3-dimethyl-3,7-dihydro-1*H*-purine-2,6-dione (10 mmol), 1-chloropropan-2-one or 2-chloro-1-phenylethan-1-one (15 mmol), potassium carbonate (30 mmol) and acetonitrile (15 mL) were refluxed for 12 h. After this time, the acetonitrile was removed *in vacuo* and the resulting residues were dissolved in dichloromethane (20 mL). The organic layers were washed with water (2 \times 20 mL) and dried over anhydrous Na₂SO₄, filtered and evaporated to dryness to give the crude products that were recrystallized from 96% ethanol (yield: 85–91%).

General procedure for the synthesis of 2-fluoro and 3-trifluoromethylphenylpiperazinyl derivatives of 1*H*-imidazo[2,1-*f*]purine-2,4(3*H*,8*H*)-dione (4–21)

A mixture of 7-ketonyl derivatives of 8-bromo-1,3-dimethyl-3,7-dihydro-1*H*-purine-2,6-dione 1–3 (5 mmol) with double amount of appropriate 2-fluoro or 3-trifluoromethylphenylpiperazinylamine (10 mmol) was refluxed in 2-methoxyethanol (20 mL) for 12 h. The solvent was removed *in vacuo*, and the obtained residue was purified by flash column chromatography on silica gel using mixture of dichloromethane/methanol (9/1) or (9/1.2) as an eluent.

8-(3-(4-(2-Fluorophenyl)piperazin-1-yl)propyl)-1,3-dimethyl-1*H*-imidazo[2,1-*f*]purine-2,4(3*H*,8*H*)-dione (4)

Yield: 62%, cream solid: m.p. 209–210 °C, $t_R = 0.831$; ¹H-NMR (300 MHz, CDCl₃): δ (ppm): 2.07–2.16 (*m*, 2H, CH₂CH₂CH₂), 2.46 (*t*, 2H, *J* = 7.3 Hz, CH₂CH₂CH₂), 2.64–2.65 (*m*, 4H, N(CH₂)₂), 3.09–3.12 (*m*, 4H, (CH₂)₂N), 3.43 (*s*, 3H, N3–CH₃), 3.59 (*s*, 3H, N1–CH₃), 4.17 (*t*, 2H, *J* = 7.4 Hz, N8–CH₂), 6.81–6.82 (*d*, 1H, *J* = 2.3 Hz, arom), 6.96–7.05 (*m*, 4H, arom), 7.39–7.40 (*d*, 1H, *J* = 2.3 Hz, C6*H*). ¹³C NMR (75 MHz, CDCl₃) δ (ppm): 26.21, 27.77, 30.07, 44.16, 46.23, 50.45, 50.49, 53.10, 54.43, 105.00, 107.39, 115.98, 116.25, 118.62, 118.86, 122.51, 124.46, 139.98, 147.43, 151.98, 154.04, 157.34. ¹⁹F NMR (282 MHz, CDCl₃): δ (ppm): –123.19 (*s*, 1F). MS (EI) *m/z*: 440.38 [M + 1]⁺. Anal. calcd for C₂₂H₂₆FN₇O₂: C, 60.12; H, 5.96; N, 22.31; found: C, 60.2; H, 6.04; N, 22.37.

8-(4-(4-(2-Fluorophenyl)piperazin-1-yl)butyl)-1,3-dimethyl-1*H*-imidazo[2,1-*f*]purine-2,4(3*H*,8*H*)-dione (5)

Yield: 69%, cream solid: m.p. 144–145 °C, $t_R = 1.011$; ¹H-NMR (300 MHz, CDCl₃): δ (ppm): 1.61–1.66 (*m*, 2H, CH₂CH₂CH₂CH₂),

1.92–2.02 (*m*, 2H, CH₂CH₂CH₂CH₂), 2.50 (*t*, 2H, *J* = 7.1 Hz, CH₂CH₂CH₂CH₂), 2.60–2.66 (*m*, 4H, N(CH₂)₂), 3.10–3.12 (*m*, 4H, (CH₂)₂N), 3.43 (*s*, 3H, N3–CH₃), 3.59 (*s*, 3H, N1–CH₃), 4.19 (*t*, 2H, *J* = 2.8 Hz, N8–CH₂), 6.78–6.79 (*d*, 1H, *J* = 2.3 Hz, arom), 6.92–7.04 (*m*, 4H, arom), 7.40–7.41 (*d*, 1H, *J* = 3 Hz, C6H). ¹³C NMR (75 MHz, CDCl₃) δ (ppm): 23.30, 26.96, 27.52, 30.09, 46.11, 46.23, 50.38, 53.24, 57.62, 100.05, 107.60, 115.96, 116.24, 117.96, 118.85, 122.49, 124.42, 135.33, 139.98, 147.46, 151.98, 157.32, 168.14. ¹⁹F NMR (282 MHz, CDCl₃): δ (ppm): –123.19 (*s*, 1F). MS (EI) *m/z*: 454.34 [M + 1]⁺. Anal. calcd for C₂₃H₂₈FN₇O₂: C, 60.91; H, 6.22; N, 21.62; found: C, 61.2; H, 6.32; N, 21.37.

*8-(5-(4-(2-Fluorophenyl)piperazin-1-yl)pentyl)-1,3-dimethyl-1*H*-imidazo[2,1-*f*]purine-2,4(3*H*,8*H*)-dione (6)*

Yield: 52%, Cream solid: m.p. 168–170 °C, *t*_R = 1.145; ¹H-NMR (300 MHz, CDCl₃): δ (ppm): 1.40–1.43 (*m*, 2H, CH₂CH₂CH₂CH₂), 1.62–1.66 (*m*, 2H, CH₂CH₂CH₂CH₂CH₂), 1.89–1.97 (*m*, 2H, CH₂CH₂CH₂CH₂CH₂), 2.45 (*t*, 2H, *J* = 2.8 Hz, CH₂CH₂CH₂CH₂CH₂), 2.60–2.68 (*m*, 4H, N(CH₂)₂), 3.10–3.14 (*m*, 4H, (CH₂)₂N), 3.43 (*s*, 3H, N3–CH₃), 3.60 (*s*, 3H, N1–CH₃), 4.07 (*t*, 2H, *J* = 7.1 Hz, N8–CH₂), 6.78–6.79 (*d*, 1H, *J* = 2.3 Hz, arom), 6.90–7.05 (*m*, 4H, arom), 7.40–7.41 (*d*, 1H, *J* = 3.1 Hz, C6H). ¹³C NMR (75 MHz, CDCl₃) δ (ppm): 24.32, 25.97, 27.75, 29.25, 30.07, 46.13, 50.23, 53.19, 58.11, 100.00, 107.52, 115.93, 116.21, 118.04, 118.89, 122.59, 124.42, 124.46, 139.94, 147.31, 151.95, 152.18, 154.01, 157.29. ¹⁹F NMR (282 MHz, CDCl₃): δ (ppm): –123.19 (*s*, 1F). MS (EI) *m/z*: 468.43 [M + 1]⁺. Anal. calcd for C₂₄H₃₀FN₇O₂: C, 61.65; H, 6.47; N, 20.97; found: C, 61.42; H, 6.66; N, 21.07.

*8-(3-(4-(2-Fluorophenyl)piperazin-1-yl)propyl)-1,3,7-trimethyl-1*H*-imidazo[2,1-*f*]purine-2,4(3*H*,8*H*)-dione (7)*

Yield: 72%, Cream solid: m.p. 160–161 °C, *t*_R = 1.005; ¹H-NMR (300 MHz, CDCl₃): δ (ppm): 2.09–2.16 (*m*, 2H, CH₂CH₂CH₂), 2.35 (*s*, 3H, CH₃), 2.45 (*t*, 2H, *J* = 2.9 Hz, CH₂CH₂CH₂), 2.63–2.65 (*m*, 4H, N(CH₂)₂), 3.09–3.12 (*m*, 4H, (CH₂)₂N), 3.42 (*s*, 3H, N3–CH₃), 3.58 (*s*, 3H, N1–CH₃), 4.10 (*t*, 2H, *J* = 7.4 Hz, N8–CH₂), 6.92–7.05 (*m*, 4H, arom), 7.26 (*s*, 1H, C6H). ¹³C NMR (75 MHz, CDCl₃) δ (ppm): 10.32, 26.01, 27.74, 30.04, 41.17, 50.43, 50.48, 53.16, 54.67, 104.43, 115.98, 116.25, 118.83, 118.88, 122.57, 124.46, 127.13, 139.88, 147.71, 151.43, 152.01, 154.02, 157.32. ¹⁹F NMR (282 MHz, CDCl₃): δ (ppm): –123.19 (*s*, 1F). MS (EI) *m/z*: 454.34 [M + 1]⁺. Anal. calcd for C₂₃H₂₈FN₇O₂: C, 60.91; H, 6.22; N, 21.62; found: C, 60.82; H, 6.41; N, 21.73.

*8-(4-(4-(2-Fluorophenyl)piperazin-1-yl)butyl)-1,3,7-trimethyl-1*H*-imidazo[2,1-*f*]purine-2,4(3*H*,8*H*)-dione (8)*

Yield: 84%, Cream solid: m.p. 153–155 °C, *t*_R = 1.155; ¹H-NMR (300 MHz, CDCl₃): δ (ppm): 1.55–1.66 (*m*, 2H, CH₂CH₂CH₂CH₂), 1.87–1.94 (*m*, 2H, CH₂CH₂CH₂CH₂), 2.33 (*s*, 3H, CH₃), 2.53–2.68 (*m*, 6H, CH₂CH₂CH₂CH₂ + N(CH₂)₂), 3.10–3.12 (*m*, 4H, (CH₂)₂N), 3.43 (*s*, 3H, N3–CH₃), 3.59 (*s*, 3H, N1–CH₃), 4.05 (*t*, 2H, *J* = 3.1 Hz, N8–CH₂), 6.93–7.05 (*m*, 4H, arom), 7.26 (*s*, 1H, C6H). ¹³C NMR (75 MHz, CDCl₃) δ (ppm): 10.41, 23.72, 24.53, 27.34, 27.74, 30.06, 43.17, 50.41, 53.25, 57.63, 58.31, 104.59, 115.96, 116.24, 118.88, 122.56, 124.42, 124.46, 126.98, 139.92, 147.77, 151.02, 151.43, 154.07. ¹⁹F NMR (282 MHz, CDCl₃): δ (ppm): –123.19 (*s*, 1F). MS (EI) *m/z*: 468.43 [M + 1]⁺. Anal. calcd for C₂₄H₃₀FN₇O₂: C, 61.65; H, 6.47; N, 20.97; found: C, 61.7; H, 6.32; N, 21.03.

*8-(5-(4-(2-Fluorophenyl)piperazin-1-yl)pentyl)-1,3,7-trimethyl-1*H*-imidazo[2,1-*f*]purine-2,4(3*H*,8*H*)-dione (9)*

Yield: 92%, Cream solid: m.p. 143–145 °C, *t*_R = 1.197; ¹H-NMR (300 MHz, CDCl₃): δ (ppm): 1.37–1.45 (*m*, 2H, CH₂CH₂CH₂CH₂CH₂), 1.57–1.65 (*m*, 2H, CH₂CH₂CH₂CH₂CH₂), 1.86–1.91 (*m*, 2H, CH₂CH₂CH₂CH₂CH₂), 2.32 (*s*, 3H, CH₃), 2.43 (*t*, 2H, *J* = 2.8 Hz, CH₂CH₂CH₂CH₂CH₂), 2.60–2.66 (*m*, 4H, N(CH₂)₂), 3.10–3.13 (*m*, 4H, (CH₂)₂N), 3.42 (*s*, 3H, N3–CH₃), 3.59 (*s*, 3H, N1–CH₃), 4.01 (*t*, 2H, *J* = 7.1 Hz, N8–CH₂), 6.91–7.16 (*m*, 4H, arom), 7.26 (*s*, 1H, C6H). ¹³C NMR (75 MHz, CDCl₃) δ (ppm): 5.67, 19.71, 21.40, 22.99, 24.52, 25.33, 38.50, 45.61, 48.51, 53.45, 95.12, 99.80, 111.19, 111.46, 114.13, 117.70, 111.81, 119.67, 122.07, 135.15, 143.01, 146.67, 147.25, 149.28, 152.57. ¹⁹F NMR (282 MHz, CDCl₃): δ (ppm): –123.19 (*s*, 1F). MS (EI) *m/z*: 482.39 [M + 1]⁺. Anal. calcd for C₂₅H₃₂FN₇O₂: C, 62.35; H, 6.7; N, 20.36; found: C, 62.42; H, 6.78; N, 20.37.

*8-(3-(4-(2-Fluorophenyl)piperazin-1-yl)propyl)-1,3-dimethyl-7-phenyl-1*H*-imidazo[2,1-*f*]purine-2,4(3*H*,8*H*)-dione (10)*

Yield: 65%, Cream oil, *t*_R = 1.232; ¹H-NMR (300 MHz, CDCl₃): δ (ppm): 1.18–1.42 (*m*, 2H, CH₂CH₂CH₂), 1.94–2.04 (*m*, 2H, CH₂CH₂CH₂), 2.53–2.73 (*m*, 4H, N(CH₂)₂), 2.96–3.12 (*m*, 4H, (CH₂)₂N), 3.32 (*s*, 3H, N3–CH₃), 3.55 (*s*, 3H, N1–CH₃), 3.63 (*t*, 2H, *J* = 4.1 Hz, N8–CH₂), 6.50–6.55 (*m*, 2H, arom), 6.93–7.00 (*m*, 3H, arom), 7.35–7.58 (*m*, 4H, arom), 7.98–8.01 (*d*, *J* = 3.4 Hz, 1H, C6H). ¹³C NMR (75 MHz, CDCl₃) δ (ppm): 24.23, 25.92, 27.80, 29.69, 30.13, 42.36, 49.32, 50.37, 50.41, 52.99, 53.41, 54.78, 105.34, 115.90, 116.18, 118.80, 118.85, 122.40, 122.51, 124.40, 124.45, 128.26, 128.39, 151.74, 152.03, 154.06, 154.25, 157.32. ¹⁹F NMR (282 MHz, CDCl₃): δ (ppm): –123.19 (*s*, 1F). MS (EI) *m/z*: 516.36 [M + 1]⁺. Anal. calcd for C₂₈H₃₀FN₇O₂: C, 65.23; H, 5.86; N, 19.02; found: C, 65.38; H, 6.08; N, 18.96.

*8-(4-(4-(2-Fluorophenyl)piperazin-1-yl)butyl)-1,3-dimethyl-7-phenyl-1*H*-imidazo[2,1-*f*]purine-2,4(3*H*,8*H*)-dione (11)*

Yield: 75%, Cream solid: m.p. 133–134 °C, *t*_R = 1.363; ¹H-NMR (300 MHz, CDCl₃): δ (ppm): 1.21–1.42 (*m*, 2H, CH₂CH₂CH₂CH₂), 1.70–1.92 (*m*, 2H, CH₂CH₂CH₂CH₂), 2.68–2.74 (*m*, 2H, CH₂CH₂CH₂CH₂), 2.86–2.92 (*m*, 4H, N(CH₂)₂), 3.08–3.16 (*m*, 4H, (CH₂)₂N), 3.32–3.39 (*m*, 4H, N3–CH₃ + N8–CH₂), 3.54–3.72 (*m*, 4H, N1–CH₃ + N8–CH₂), 6.80–7.05 (*m*, 5H, arom), 7.45–7.63 (*m*, 4H, arom), 8.04–8.06 (*d*, *J* = 8.0 Hz, 1H, C6H). ¹³C NMR (75 MHz, CDCl₃) δ (ppm): 23.30, 24.96, 27.52, 29.69, 30.90, 42.89, 49.26, 49.67, 57.68, 59.07, 60.90, 71.92, 115.98, 116.25, 118.92, 119.20, 122.78, 122.89, 124.45, 124.49, 127.38, 127.70, 128.08, 128.71, 128.87, 134.32, 149.19, 151.74, 154.19. ¹⁹F NMR (282 MHz, CDCl₃): δ (ppm): –123.19 (*s*, 1F). MS (EI) *m/z*: 530.60 [M + 1]⁺. Anal. calcd for C₂₉H₃₂FN₇O₂: C, 65.75; H, 6.09; N, 18.51; found: C, 65.73; H, 6.02; N, 18.53.

*8-(5-(4-(2-Fluorophenyl)piperazin-1-yl)pentyl)-1,3-dimethyl-7-phenyl-1*H*-imidazo[2,1-*f*]purine-2,4(3*H*,8*H*)-dione (12)*

Yield: 77%, Cream oil, *t*_R = 1.422; ¹H-NMR (300 MHz, CDCl₃): δ (ppm): 1.19–1.28 (*m*, 2H, CH₂CH₂CH₂CH₂CH₂), 1.40–1.45 (*m*, 2H, CH₂CH₂CH₂CH₂CH₂), 1.75–1.80 (*m*, 2H, CH₂CH₂CH₂CH₂CH₂), 2.31 (*t*, 2H, *J* = 2.2 Hz, CH₂CH₂CH₂CH₂CH₂), 2.57–2.63 (*m*, 4H, N(CH₂)₂), 3.07–3.14 (*m*, 4H, (CH₂)₂N), 3.44 (*s*, 3H, N3–CH₃), 3.63 (*s*, 3H, N1–CH₃), 4.11 (*t*, 2H, *J* = 3.4 Hz, N8–CH₂), 6.91–7.05 (*m*, 5H, arom), 7.41–7.50 (*m*, 4H, arom), 8.04–8.03 (*d*, *J* = 5.0 Hz, 1H, C6H). ¹³C NMR (75 MHz, CDCl₃) δ (ppm): 23.30, 24.96, 27.52, 29.69, 30.90, 42.89, 49.26, 49.67, 52.99, 57.68, 59.07, 60.90, 71.92, 115.98, 116.25, 118.92, 119.20, 122.78, 122.89, 124.45, 124.49, 127.38, 127.70, 128.08, 128.71, 128.87, 134.32, 149.19, 151.74, 154.19. ¹⁹F NMR (282 MHz,

CDCl_3 : δ (ppm): -123.14 (s, 1F). MS (EI) m/z : 544.55 $[\text{M} + 1]^+$. Anal. calcd for $\text{C}_{30}\text{H}_{34}\text{FN}_7\text{O}_2$: C, 66.28; H, 6.30; N, 18.04; found: C, 66.42; H, 6.06; N, 18.07.

1,3-Dimethyl-8-(3-(4-(3-(trifluoromethyl)phenyl)piperazin-1-yl)propyl)-1H-imidazo[2,1-f]purine-2,4(3H,8H)-dione (13)

Yield: 78%, Cream solid: m.p. $110\text{--}112^\circ\text{C}$, $t_{\text{R}} = 1.211$; $^1\text{H-NMR}$ (300 MHz, CDCl_3): δ (ppm): $2.09\text{--}2.18$ (m, 2H, $\text{CH}_2\text{CH}_2\text{CH}_2$), 2.46 (t, 2H, $J = 7.3$ Hz, $\text{CH}_2\text{CH}_2\text{CH}_2$), $2.64\text{--}2.65$ (m, 4H, $\text{N}(\text{CH}_2)_2$), $3.24\text{--}3.27$ (m, 4H, $(\text{CH}_2)_2\text{N}$), 3.43 (s, 3H, N3-CH_3), 3.60 (s, 3H, N1-CH_3), 4.18 (t, 2H, $J = 3.3$ Hz, N8-CH_2), $6.82\text{--}6.83$ (m, 2H, arom), $7.04\text{--}7.10$ (m, 3H, arom), $7.40\text{--}7.41$ (d, 1H, $J = 2.3$ Hz, C6H). $^{13}\text{C NMR}$ (75 MHz, CDCl_3) δ (ppm): 26.96 , 27.52 , 30.09 , 42.16 , 46.75 , 50.45 , 50.49 , 52.99 , 54.43 , 105.00 , 107.39 , 111.37 , 115.09 , 116.25 , 117.22 , 121.01 , 122.51 , 124.16 , 129.53 , 131.21 , 151.28 , 152.01 , 154.04 . $^{19}\text{F NMR}$ (282 MHz, CDCl_3): δ (ppm): -60.34 (s, 3F). MS (EI) m/z : 490.36 $[\text{M} + 1]^+$. Anal. calcd for $\text{C}_{23}\text{H}_{26}\text{F}_3\text{N}_7\text{O}_2$: C, 56.44; H, 5.35; N, 20.03; found: C, 56.20; H, 5.30; N, 20.37.

1,3-Dimethyl-8-(4-(4-(3-(trifluoromethyl)phenyl)piperazin-1-yl)butyl)-1H-imidazo[2,1-f]purine-2,4(3H,8H)-dione (14)

Yield: 82%, Cream solid: m.p. $170\text{--}171^\circ\text{C}$, $t_{\text{R}} = 1.254$; $^1\text{H-NMR}$ (300 MHz, CDCl_3): δ (ppm): $1.48\text{--}1.53$ (m, 2H, $\text{CH}_2\text{CH}_2\text{CH}_2\text{CH}_2$), $1.82\text{--}1.92$ (m, 2H, $\text{CH}_2\text{CH}_2\text{CH}_2\text{CH}_2$), $2.40\text{--}2.54$ (m, 6H, $\text{CH}_2\text{CH}_2\text{CH}_2\text{CH}_2 + \text{N}(\text{CH}_2)_2$), $3.10\text{--}3.17$ (m, 4H, $(\text{CH}_2)_2\text{N}$), 3.34 (s, 3H, N3-CH_3), 3.51 (s, 3H, N1-CH_3), 4.04 (t, 2H, $J = 3.1$ Hz, N8-CH_2), $6.79\text{--}6.80$ (d, 1H, $J = 2.3$ Hz, arom), $6.91\text{--}7.01$ (m, 2H, arom), $7.24\text{--}7.26$ (m, 2H, arom), $7.40\text{--}7.41$ (d, 1H, $J = 3$ Hz, C6H). $^{13}\text{C NMR}$ (75 MHz, CDCl_3) δ (ppm): 26.96 , 27.52 , 29.69 , 30.09 , 42.16 , 46.75 , 50.45 , 50.49 , 52.99 , 54.43 , 105.00 , 107.39 , 112.22 , 115.75 , 115.98 , 117.92 , 118.62 , 121.01 , 123.56 , 129.53 , 129.91 , 151.28 , 152.01 , 154.04 . $^{19}\text{F NMR}$ (282 MHz, CDCl_3): δ (ppm): -62.99 (s, 3F). MS (EI) m/z : 504.10 $[\text{M} + 1]^+$. Anal. calcd for $\text{C}_{24}\text{H}_{28}\text{F}_3\text{N}_7\text{O}_2$: C, 57.25; H, 5.61; N, 19.47; found: C, 57.02; H, 5.32; N, 19.37.

1,3-Dimethyl-8-(5-(4-(3-(trifluoromethyl)phenyl)piperazin-1-yl)pentyl)-1H-imidazo[2,1-f]purine-2,4(3H,8H)-dione (15)

Yield: 86%, Cream oil, $t_{\text{R}} = 1.301$, $^1\text{H-NMR}$ (300 MHz, CDCl_3): δ (ppm): $1.40\text{--}1.42$ (m, 2H, $\text{CH}_2\text{CH}_2\text{CH}_2\text{CH}_2\text{CH}_2$), $1.62\text{--}1.67$ (m, 2H, $\text{CH}_2\text{CH}_2\text{CH}_2\text{CH}_2\text{CH}_2$), $1.89\text{--}1.96$ (m, 2H, $\text{CH}_2\text{CH}_2\text{CH}_2\text{CH}_2\text{CH}_2$), 2.49 (t, 2H, $J = 2.8$ Hz, $\text{CH}_2\text{CH}_2\text{CH}_2\text{CH}_2\text{CH}_2$), $2.70\text{--}2.73$ (m, 4H, $\text{N}(\text{CH}_2)_2$), $3.26\text{--}3.28$ (m, 4H, $(\text{CH}_2)_2\text{N}$), 3.43 (s, 3H, N3-CH_3), 3.59 (s, 3H, N1-CH_3), 4.06 (t, 2H, $J = 7.1$ Hz, N8-CH_2), $6.78\text{--}6.79$ (d, 1H, $J = 2.3$ Hz, arom), $7.05\text{--}7.09$ (m, 4H, arom), $7.40\text{--}7.41$ (d, 1H, $J = 3.1$ Hz, C6H). $^{13}\text{C NMR}$ (75 MHz, CDCl_3) δ (ppm): 26.96 , 27.52 , 28.33 , 29.69 , 30.09 , 42.16 , 46.75 , 50.45 , 50.49 , 52.99 , 54.43 , 105.00 , 107.39 , 111.97 , 114.89 , 116.25 , 118.02 , 121.01 , 122.96 , 124.56 , 129.53 , 131.42 , 151.28 , 152.01 , 154.04 . $^{19}\text{F NMR}$ (282 MHz, CDCl_3): δ (ppm): -63.14 (s, 3F). MS (EI) m/z : 518.19 $[\text{M} + 1]^+$. Anal. calcd for $\text{C}_{25}\text{H}_{30}\text{F}_3\text{N}_7\text{O}_2$: C, 58.02; H, 5.84; N, 18.94; found: C, 58.22; H, 5.77; N, 18.97.

1,3,7-Trimethyl-8-(3-(4-(3-(trifluoromethyl)phenyl)piperazin-1-yl)propyl)-1H-imidazo[2,1-f]purine-2,4(3H,8H)-dione (16)

Yield: 95%, Cream oil, $t_{\text{R}} = 1.172$; $^1\text{H-NMR}$ (300 MHz, CDCl_3): δ (ppm): $2.11\text{--}2.13$ (m, 2H, $\text{CH}_2\text{CH}_2\text{CH}_2$), 2.34 (s, 3H, CH_3), $2.47\text{--}2.49$ (m, 2H, $\text{CH}_2\text{CH}_2\text{CH}_2$), $2.64\text{--}2.65$ (m, 4H, $\text{N}(\text{CH}_2)_2$), $3.23\text{--}3.26$ (m, 4H, $(\text{CH}_2)_2\text{N}$), 3.43 (s, 3H, N3-CH_3), 3.58 (s, 3H, N1-CH_3), 4.10 (t, 2H, $J = 3.3$ Hz, N8-CH_2), $7.03\text{--}7.16$ (m, 4H, arom), $7.34\text{--}7.37$ (m, 1H, C6H). $^{13}\text{C NMR}$ (75 MHz, CDCl_3) δ (ppm): 10.30 , 26.96 , 27.52 , 28.33 , 30.09 , 42.16 , 46.75 , 50.45 ,

50.49 , 52.99 , 54.43 , 105.00 , 107.23 , 112.07 , 115.89 , 118.32 , 121.01 , 123.36 , 124.56 , 129.53 , 131.21 , 151.28 , 152.01 , 154.04 . $^{19}\text{F NMR}$ (282 MHz, CDCl_3): δ (ppm): -60.34 (s, 3F). MS (EI) m/z : 504.39 $[\text{M} + 1]^+$. Anal. calcd for $\text{C}_{24}\text{H}_{28}\text{F}_3\text{N}_7\text{O}_2$: C, 57.25; H, 5.61; N, 19.47; found: C, 57.20; H, 5.30; N, 19.37.

1,3,7-Trimethyl-8-(4-(4-(3-(trifluoromethyl)phenyl)piperazin-1-yl)butyl)-1H-imidazo[2,1-f]purine-2,4(3H,8H)-dione (17)

Yield: 87%, Cream solid: m.p. $188\text{--}190^\circ\text{C}$, $t_{\text{R}} = 1.306$; $^1\text{H-NMR}$ (300 MHz, CDCl_3): δ (ppm): $1.48\text{--}1.53$ (m, 2H, $\text{CH}_2\text{CH}_2\text{CH}_2\text{CH}_2$), $1.76\text{--}1.78$ (m, 2H, $\text{CH}_2\text{CH}_2\text{CH}_2\text{CH}_2$), $2.24\text{--}2.51$ (m, 9H, $\text{CH}_3 + \text{CH}_2\text{CH}_2\text{CH}_2\text{CH}_2 + \text{N}(\text{CH}_2)_2$), $3.10\text{--}3.13$ (m, 4H, $(\text{CH}_2)_2\text{N}$), 3.30 (s, 3H, N3-CH_3), 3.48 (s, 3H, N1-CH_3), $3.94\text{--}3.98$ (m, 2H, N8-CH_2), $6.95\text{--}6.98$ (m, 3H, arom), $7.13\text{--}7.25$ (m, 2H, arom). $^{13}\text{C NMR}$ (75 MHz, CDCl_3) δ (ppm): 13.30 , 26.96 , 27.52 , 28.33 , 29.69 , 30.09 , 42.89 , 49.26 , 49.67 , 57.68 , 59.07 , 71.92 , 104.61 , 107.33 , 109.2 , 111.77 , 116.09 , 118.12 , 121.01 , 123.36 , 129.53 , 131.21 , 151.28 , 152.01 , 154.04 . $^{19}\text{F NMR}$ (282 MHz, CDCl_3): δ (ppm): -63.12 (s, 3F). MS (EI) m/z : 519.12 $[\text{M} + 1]^+$. Anal. calcd for $\text{C}_{25}\text{H}_{30}\text{F}_3\text{N}_7\text{O}_2$: C, 58.02; H, 5.84; N, 18.94; found: C, 58.22; H, 5.58; N, 19.07.

1,3,7-Trimethyl-8-(5-(4-(3-(trifluoromethyl)phenyl)piperazin-1-yl)pentyl)-1H-imidazo[2,1-f]purine-2,4(3H,8H)-dione (18)

Yield: 80%, Cream solid: m.p. $168\text{--}169^\circ\text{C}$, $t_{\text{R}} = 1.340$, $^1\text{H-NMR}$ (300 MHz, CDCl_3): δ (ppm): $1.35\text{--}1.37$ (m, 2H, $\text{CH}_2\text{CH}_2\text{CH}_2\text{CH}_2$), $1.55\text{--}1.58$ (m, 2H, $\text{CH}_2\text{CH}_2\text{CH}_2\text{CH}_2\text{CH}_2$), $1.83\text{--}1.85$ (m, 2H, $\text{CH}_2\text{CH}_2\text{CH}_2\text{CH}_2\text{CH}_2$), $2.28\text{--}2.93$ (m, 9H, $\text{CH}_3 + \text{CH}_2\text{CH}_2\text{CH}_2\text{CH}_2\text{CH}_2 + \text{N}(\text{CH}_2)_2$), $3.20\text{--}3.24$ (m, 4H, $(\text{CH}_2)_2\text{N}$), 3.36 (s, 3H, N3-CH_3), 3.54 (s, 3H, N1-CH_3), $3.95\text{--}4.00$ (m, 2H, N8-CH_2), $6.99\text{--}7.07$ (m, 3H, arom), $7.26\text{--}7.32$ (m, 2H, arom). $^{13}\text{C NMR}$ (75 MHz, CDCl_3) δ (ppm): 10.20 , 24.38 , 25.91 , 27.74 , 29.25 , 30.00 , 43.21 , 49.10 , 52.84 , 58.12 , 99.83 , 104.65 , 112.13 , 116.04 , 118.76 , 122.39 , 126.00 , 127.21 , 129.51 , 131.10 , 131.51 , 147.63 , 151.08 , 151.38 , 151.90 , 154.04 . $^{19}\text{F NMR}$ (282 MHz, CDCl_3): δ (ppm): -63.14 (s, 3F). MS (EI) m/z : 532.15 $[\text{M} + 1]^+$. Anal. calcd for $\text{C}_{26}\text{H}_{32}\text{F}_3\text{N}_7\text{O}_2$: C, 58.75; H, 6.07; N, 18.44; found: C, 58.52; H, 6.10; N, 18.50.

1,3-Dimethyl-7-phenyl-8-(3-(4-(3-(trifluoromethyl)phenyl)piperazin-1-yl)propyl)-1H-imidazo[2,1-f]purine-2,4(3H,8H)-dione (19)

Yield: 79%, Cream solid: m.p. $128\text{--}129^\circ\text{C}$, $t_{\text{R}} = 1.501$; $^1\text{H-NMR}$ (300 MHz, CDCl_3): δ (ppm): $1.82\text{--}2.02$ (m, 2H, $\text{CH}_2\text{CH}_2\text{CH}_2$), 2.34 (t, 2H, $J = 7.3$ Hz, $\text{CH}_2\text{CH}_2\text{CH}_2$), $2.42\text{--}2.44$ (m, 4H, $\text{N}(\text{CH}_2)_2$), $3.08\text{--}3.11$ (m, 4H, $(\text{CH}_2)_2\text{N}$), 3.45 (s, 3H, N3-CH_3), 3.63 (s, 3H, N1-CH_3), 4.21 (t, 2H, $J = 3.3$ Hz, N8-CH_2), $6.90\text{--}7.08$ (m, 6H, arom), $7.33\text{--}7.49$ (m, 4H, arom). $^{13}\text{C NMR}$ (75 MHz, CDCl_3) δ (ppm): 10.30 , 25.92 , 27.80 , 29.69 , 30.13 , 42.36 , 49.32 , 50.37 , 50.41 , 52.99 , 53.41 , 54.78 , 105.34 , 112.07 , 115.90 , 116.18 , 118.32 , 121.01 , 122.40 , 124.40 , 125.22 , 128.26 , 129.53 , 131.21 , 151.28 , 152.01 , 154.04 , 154.25 , 157.32 . $^{19}\text{F NMR}$ (282 MHz, CDCl_3): δ (ppm): -60.34 (s, 3F). MS (EI) m/z : 566.49 $[\text{M} + 1]^+$. Anal. calcd for $\text{C}_{29}\text{H}_{30}\text{F}_3\text{N}_7\text{O}_2$: C, 61.58; H, 5.35; N, 17.34; found: C, 61.60; H, 5.33; N, 17.43.

1,3-Dimethyl-7-phenyl-8-(4-(4-(3-(trifluoromethyl)phenyl)piperazin-1-yl)butyl)-1H-imidazo[2,1-f]purine-2,4(3H,8H)-dione (20)

Yield: 81%, Cream oil; $t_{\text{R}} = 1.490$; $^1\text{H-NMR}$ (300 MHz, CDCl_3): δ (ppm): $1.18\text{--}1.25$ (m, 4H, $\text{CH}_2\text{CH}_2\text{CH}_2\text{CH}_2$), $1.42\text{--}1.52$ (m, 6H, $\text{CH}_2\text{CH}_2\text{CH}_2\text{CH}_2 + \text{N}(\text{CH}_2)_2$), $3.39\text{--}3.64$ (m, 10H, $(\text{CH}_2)_2\text{N} + \text{N3-CH}_3 + \text{N1-CH}_3$), 4.16 (t, 2H, $J = 3.1$ Hz, N8-CH_2), $7.09\text{--}7.25$ (m, 2H, arom), $7.43\text{--}7.52$ (m, 8H, arom). $^{13}\text{C NMR}$ (75 MHz, CDCl_3) δ (ppm): 22.97 , 24.96 , 27.52 , 29.96 , 30.89 , 42.15 , 49.26 , 49.77 , 57.68 , 59.17 , 60.94 , 72.02 ,

111.87, 115.91, 116.27, 119.12, 120.99, 122.87, 122.89, 124.54, 125.01, 128.08, 128.71, 128.87, 129.53, 131.01, 149.23, 151.18, 152.17, 154.01. ¹⁹F NMR (282 MHz, CDCl₃): δ (ppm): -62.82 (*s*, 3F). MS (EI) *m/z*: 580.14 [M+1]⁺. Anal. calcd for C₃₀H₃₂F₃N₇O₂: C, 62.17; H, 5.56; N, 16.92; found: C, 62.02; H, 5.32; N, 16.73.

*1,3-Dimethyl-7-phenyl-8-(5-(4-(3-(trifluoromethyl)phenyl)piperazin-1-yl)pentyl)-1*H*-imidazo[2,1-*f*]purine-2,4(3*H*,8*H*)-dione (21)*

Yield: 85%, Cream oil, *t_R* = 1.540, ¹H-NMR (300 MHz, CDCl₃): δ (ppm): 1.18–1.25 (*m*, 4H, CH₂CH₂CH₂CH₂CH₂), 1.56–1.81 (*m*, 8H, CH₂CH₂CH₂CH₂CH₂+N(CH₂)₂), 3.36–3.63 (*m*, 10H, (CH₂)₂N+N3-CH₃+N1-CH₃), 4.10–4.12 (*m*, 2H, N8-CH₂), 7.10–7.25 (*m*, 2H, arom), 7.42–7.64 (*m*, 8H, arom). ¹³C NMR (75 MHz, CDCl₃) δ (ppm): 23.33, 24.96, 27.52, 29.69, 30.90, 42.89, 49.26, 49.67, 52.99, 57.68, 59.07, 60.90, 71.92, 112.07, 115.89, 116.25, 118.32, 119.20, 121.01, 122.78, 122.89, 123.36, 128.08, 128.71, 128.87, 129.53, 131.21, 149.19, 151.28, 152.01, 154.04. ¹⁹F NMR (282 MHz, CDCl₃): δ (ppm): -62.81 (*s*, 3F). MS (EI) *m/z*: 594.27 [M+1]⁺. Anal. calcd for C₃₁H₃₄F₃N₇O₂: C, 62.72; H, 5.77; N, 16.52; found: C, 62.61; H, 5.71; N, 16.67.

Radioligand binding assays

All of the compounds were tested in radioligand binding assays measuring their affinity for 5-HT_{1A} and 5-HT₇ receptors. The inhibition constants *K_i* were determined based on previously described protocols^{29,32}. One millimolar stock solutions of the compounds to be tested was prepared in DMSO. Serial dilutions of compounds were prepared in 96-well microplate in assay buffers using an automated pipetting system (epMotion 5070; Eppendorf). Radioligand binding was performed using cryopreserved membranes from cells stably expressing the relevant human receptor. Reagents and condition: 50 μL working solution of the tested compounds, 50 μL radioligand solution and 150 μL diluted membranes prepared in assay buffer were transferred to 96-well microplates. These were covered with sealing tape, mixed and incubated. The reaction was terminated by rapid filtration through UniFilter 96 GF/B filter microplate and 10 rapid washes with 200 μL 50 mM Tris buffer (4 °C, pH 7.4) were performed using vacuum manifold and 96-well pipettor. The UniFilter microplates were dried overnight at 37 °C in dry incubator. The UniFilter bottoms were sealed and 30 μL of liquid scintillator Betaplate Scint (PerkinElmer, Waltham, MA) was added to each well. The plates were allowed to equilibrate for 1 h, and then, radioactivity was counted in MicroBeta TriLux 1450 scintillation counter (PerkinElmer, Waltham, MA) at approximately 30% efficiency. Data were fitted to a one-site curve-fitting equation with Prism 5 (GraphPad Software Inc., La Jolla, CA) and *K_i* values were calculated using the Cheng–Prusoff equation³³. Each compound was tested in 10 concentrations from 1 × 10⁻⁵ M to 1 × 10⁻⁹ M (final concentration). All the assays were carried out in duplicates (*n* = 2). The inhibition constants *K_i* for D₂ and 5-HT_{2A,6} receptors were determined based on previously described protocols^{29,32}.

The phosphodiesterase activity tests

Inhibition of PDE4B1 and PDE10A was measured using PDElight HTS cAMP phosphodiesterase assay kit (PDElight™, Lonza) according to manufacturer's recommendations. The percentage of inhibition was calculated to vehicle control (DMSO). Test and reference compounds were dissolved in dimethyl sulfoxide (DMSO) at a concentration of 1 mM and further diluted in assay buffer (10 mM Tris-HCl, 10 mM magnesium chloride and 0.05% Tween-20; pH 7.4) and eight concentrations were tested.

Inhibition of PDE4B1 and PDE10A was measured using PDElight HTS cAMP phosphodiesterase assay kit (Lonza) according to the manufacturer's recommendations. About 5 ng of human, recombinant PDE4B1 (Sigma-Aldrich, St. Louis, MO) or 10 ng PDE10A (BPS Biosciences) in assay buffer was incubated with reference (papaverine for PDE10A, 3-isobutyl-1-methylxanthine (IBMX) for PDE4B1) and tested compound for 20 min. After incubation, the cAMP substrate (final concentration 1.25 μM for PDE10A and 10 μM for PDE4B1) was added and incubated for 1 h. Then, PDElight AMP detection reagent was added and incubated 10 min. All reactions were carried out at 37 °C in white-walled, 384-well plate. Luminescence was measured in a multifunctional microplate reader (POLARstar Omega, BMG Labtech, Germany). All the assays were carried out in duplicates (*n* = 2).

Functional assays for 5-HT_{1A} and 5-HT₇ receptors

Test and reference compounds were dissolved in dimethyl sulfoxide (DMSO) at a concentration of 1 mM. Serial dilutions were prepared in 96-well microplate in assay buffers and eight concentrations were tested. All the assays were carried out in duplicates (*n* = 2). The EC₅₀ values (concentration producing a half-maximal response) and IC₅₀ values (concentration causing a half-maximal inhibition of the control agonist response) were determined by nonlinear regression analysis of the concentration response curves generated with mean replicate values using Hill equation curve fitting (GraphPad Prism 6.0 software; GraphPad Software Inc., La Jolla, CA). The log IC₅₀ was used to obtain the antagonist equilibrium dissociation constant (*K_b*) by applying the Cheng–Prusoff Equation (1):

$$K_b = \frac{IC_{50}}{1 + \left(\frac{A}{EC_{50A}}\right)} \quad (1)$$

where *K_b* – antagonist equilibrium dissociation constant, A – concentration of reference agonist in the assay, EC_{50A} = EC₅₀ value of reference agonist.

A cellular aequorin-based functional assay was performed with recombinant CHO-K1 cells expressing mitochondrially targeted aequorin, human GPRC and the promiscuous G protein α16 for 5-HT_{1A}. Assay was executed according to previously described protocol³⁴. After thawing, cells were transferred to (DMEM/HAM's F12 with 0.1% protease-free BSA) and centrifuged. The cell pellet was resuspended in assay buffer and coelenterazine h was added at final concentration of 5 μM. The cell suspension was incubated at 16 °C, protected from light with constant agitation for 16 h and diluted with assay buffer to the concentration of 100 000 cells/ml. after 1 h of incubation, 50 μM of the cells suspension was dispensed using automatic injectors built into the radiometric and luminescence plate counter MicroBeta2 LumiJET (PerkinElmer, Waltham, MA) into white opaque 96-well microplate preloaded with test compounds. Immediate light emission generated following calcium mobilization was recorded for 30 s. In antagonist mode, after 25 min of incubation, the reference agonist was added to the above assay mix and light emission was recorded again. Final concentration of the reference agonist was to EC80 (100 nM for serotonin).

For the 5-HT₇ receptor, adenylyl cyclase activity was monitored using cryopreserved CHO-K1 cells, expressing the human serotonin 5-HT₇ receptor. Thawed cells were resuspended in stimulation buffer (HBSS, 5 mM HEPES, 0.5 IBMX and 0.1% BSA at pH 7.4) at 200 000 cells/mL. Ten microliters of cell suspension was added to 10 μL of tested compounds and loaded onto a white opaque half area 96-well microplate. An antagonist response experiment was performed with 10 nM serotonin as the

reference agonist, and the agonist and antagonist were added simultaneously. Cell stimulation was performed for 60 min at room temperature. After incubation, cAMP measurements were taken with homogeneous time-resolved fluorescence energy transfer (TR-FRET) immunoassay using the LANCE Ultra cAMP kit (PerkinElmer, Waltham, MA). Ten microliters of EucAMP tracer working solution and 10 μ L of ULight-anti-cAMP tracer working solution were added, mixed and incubated for 1 h. The TR-FRET signal was read on an EnVision microplate reader (PerkinElmer, Waltham, MA).

Determination of lipophilicity

Borate-phosphate buffer pH 7.0 with SDS (100 mM + 50 mM + 50 mM), SDS, 0.1 M of sodium hydroxide were purchased from Sigma-Aldrich (Poznań, Poland). Methanol (MeOH) HPLC purity. Reference drugs (purity > 99.5%) were purchased from different sources: barbital, phenobarbital (Polfa-Tarchomin, Poland), aminophenazone, caffeine (Polfa-Pabianice, Poland), chloramphenicol (Polfa-Kraków, Poland), phenytoin (Polfa-Warszawa, Poland), phenacetin (Azienda Chimica e Farmaceutica, Italy), benzocaine (Alfa Aesar, Germany), procaine (Amara Co., Poland). Trazodone was extracted from Trittico CR tablets (Aziende Chimiche Riunite Angelini Francesco (A.C.R.A.F.), Italy). The analyses were performed on Beckman P/ACE MDQ instrument (Beckman, Brea, CA) with DAD with UV detection at 220 nm. The electropherograms were recorded and analyzed with the 32 Karat Software version 8.0. Uncoated fused-silica capillaries (Beckman, Brea, CA; 39 cm distance to the detector, 50 μ m internal diameter, 49 cm total length, 375 μ m external diameter) were used. Background electrolyte, samples preparation and separation conditions were prepared according to methods of Bajda et al.³⁵.

The logarithm of retention factor, $\log k$, was calculated from the MEKC migration times according to the Equation (2)³⁵:

$$\log k = \log \frac{t_R - t_{EOF}}{t_{EOF} \times \frac{t_R}{t_{MC}}} \quad (2)$$

where t_R , t_{EOF} and t_{MC} are the migration time (min) of the solute, the EOF marker (MeOH) and the micelle marker (Sudan III), respectively. Estimated $\log p$ (cLog p) coefficients for the tested compounds were calculated from calibration curve obtained by linear regression of the $\log k$ and $\log p$ values of reference compounds according to Equation (3), where parameters b and a represent the slope and intercept of the curve, respectively:

$$\log P = b \log k + a \quad (3)$$

Metabolism study

Human liver microsomes (HLMs, microsomes from liver, pooled, from human adult male and female), NADPH-regenerating system components and pentoxifylline were purchased from Sigma Aldrich (Poznań, Poland). Stock solutions of test compounds were prepared in ethanol. The final ethanol concentration in the incubation mixture was 0.38%. The incubation systems were composed of test compound (20 μ M), HLMs (0.4 mg/mL), NADPH-regenerating system and potassium phosphate buffer (100 mM, pH 7.4). NADPH-regenerating system contained NADP, glucose-6-phosphate, glucose-6-phosphate dehydrogenase and potassium phosphate buffer (100 mM, pH 7.4). Firstly, the mixtures containing HLM, the test compound and a buffer were preincubated at 37 °C for 15 min before the addition of the NADPH-regenerating system. The resulting mixture was incubated for 15 min at 37 °C in a thermoblock. Next, pentoxifylline (20 μ M, internal standard) was added, and the reaction was

stopped by the addition of perchloric acid (69–72%, by volume). Proteins were sedimented by centrifugation. The supernatant was analyzed using UPLC/MS (Waters Corporation, Milford, MA) for qualitative analysis. The peak area ratios of analyte versus internal standard were used to calculate the % remaining at the end of 15 min of biotransformation. All the assays were carried out in duplicates ($n = 2$).

Pharmacology – general condition

The experiments were performed on male Albino Swiss mice (22–28 g). The animals were kept at a room temperature of 20 ± 1 °C and had free access to food (standard laboratory pellets) and tap water before the experiment. All the experiments were conducted in the light phase between 9 a.m. and 2 p.m. All the experimental procedures were approved by the Local Ethics Commission for Animal Experiments of Jagiellonian University in Cracow. Citalopram (Sigma-Aldrich, St. Louis, MO) was dissolved in distilled water. The investigated compound (**9**) and diazepam were suspended in a 1% aqueous solution of Tween 80 and was injected intraperitoneally (ip) 60 min before the test (citalopram 30 min before the test). Each experimental group consisted of six to ten animals, and all the animals were used only once.

Forced swim (porsolt) test in swiss albino mice

The experiment was carried out according to the method of Porsolt et al.³⁷. Mice were individually placed in a glass cylinder (25 cm high; 10 cm in diameter) containing 10 cm of water maintained at 23–25 °C and were left there for 6 min. A mouse was regarded as immobile when it remained floating on the water, making only small movements to keep its head above it. The total duration of immobility was recorded during the last 4 min of a 6-min test session.

Four-plate test in Swiss albino mice

The four-plate apparatus (BIOSEB) consists of a plastic cage (25 \times 18 \times 16 cm) floored by four identical rectangular metal plates (8 \times 11 cm) separated from one another by a gap of 4 mm. The top of the cage is covered by a transparent Perspex lid that prevents escape behavior. The plates are connected to a device that can generate electric shocks. Following a 15-s habituation period, the animal's motivation to explore a novel environment was suppressed by an electric foot shock (0.8 mA, 0.5 s) every time it moves from one plate to another during a 1-min test session. This action is referred to as a ‘‘punished crossing’’ and was followed by a 3-s shock interval, during which the animal can move across plates without receiving a shock³⁸. The number of punished crossings received by an animal was recorded during the 60-s period.

Spontaneous locomotor activity in mice

Locomotor activity was recorded with an Opto M3 multichannel activity monitor (MultiDevice Software v.1.3, Columbus Instruments). Swiss albino mice were individually placed in plastic cages (22 \times 12 \times 13 cm) for 30-min habituation period, and then, the ambulation was counted from 2 to 6 min or for 1 min 15 s, that is the time equal to the observation period in the forced swim test or the four-plate test, respectively. The cages were cleaned up with 70% ethanol after each mouse.

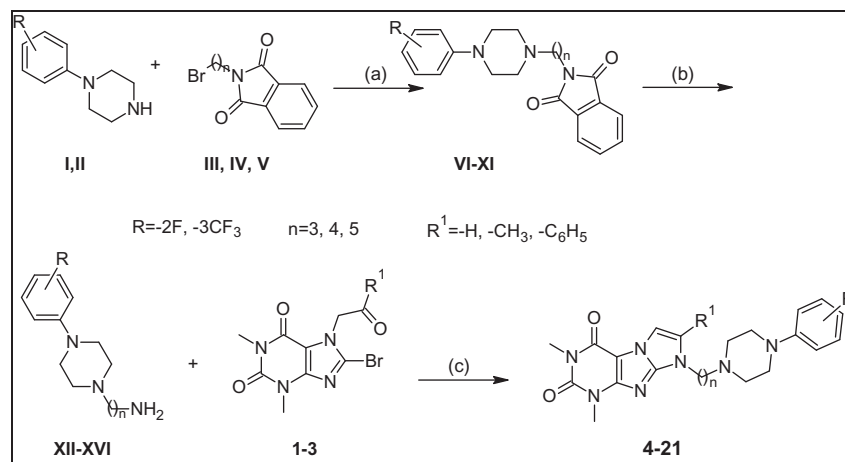
Statistics

All the data are presented as the mean \pm SEM. The statistical significance of results was evaluated by a one-way analysis of variance (ANOVA) followed by Bonferroni's comparison test. $p < 0.05$ was considered statistically significant.

Molecular modeling

The homology models of human 5-HT_{1A} and 5-HT₇ serotonin receptors adopted for docking in the present study were built on the template of β_2 adrenergic receptor crystal structure (PDB ID: 2RH1). The homology models were generated using thoroughly tested method²⁹ and were described in previously published papers^{34,39–41}. Sequence alignments between target receptors (UniProt database accession numbers P08908 and P34969, respectively) and the template were performed by hhsearch tool via GeneSilico Metaserver⁴². The crude receptor models were obtained using SwissModel⁴³ and were validated by processing in Protein Preparation Wizard. For each receptor type, a set of bioactive compounds was selected for ligand-steered binding site optimization, which was performed using induced fit docking (IFD) workflow⁴⁴. The procedure resulted in a variety of comparative models, mirroring conformational plasticity of the protein. Ligand structures were optimized using LigPrep tool and were docked to the target models using Glide XP-docking procedure, setting flexible docking option, retaining ring conformations and nitrogen inversions as were selected in the previous step. H-bond constraints and centroid of a grid box (22 × 22 × 22 Å) for docking studies were located on Asp3.32. The remaining parameters were default. Physicochemical (PSA) and ADME (QPPMDCK) properties were calculated with use of QikProp module. Glide, induced fit docking, LigPrep, Protein Preparation Wizard and QikProp were implemented in Small-Molecule Drug Discovery Suite

Scheme 1. General method for synthesis of compounds **4–21**^a.



	4	5	6	7	8	9	10	11	12
R	2-F	2-F	2-F	2-F	2-F	2-F	2-F	2-F	2-F
R¹	H	H	H	CH ₃	CH ₃	CH ₃	C ₆ H ₅	C ₆ H ₅	C ₆ H ₅
n	3	4	5	3	4	5	3	4	5

	13	14	15	16	17	18	19	20	21
R	3-CF ₃	3-CF ₃	3-CF ₃						
R¹	H	H	H	CH ₃	CH ₃	CH ₃	C ₆ H ₅	C ₆ H ₅	C ₆ H ₅
n	3	4	5	3	4	5	3	4	5

^areagents and conditions (a) K₂CO₃, KI, CH₃CN, 82 °C, 48h; (b) hydrazine monohydrate 65%, EtOH, reflux; (c) 2-methoxyethanol, reflux, 12h.

(Schrödinger, Inc.), which was licensed for Jagiellonian University Medical College.

Results and discussion

Chemistry

Following our previously developed route, the final derivatives of 1,3-dimethyl-(1*H*,8*H*)-imidazo[2,1-*f*]purine-2,4-dione (**4–21**) were achieved in via multistep synthesis. In order to carry out the process, two series of synthons were necessary: 7-ketonyl derivatives of 8-bromotheophylline (**1–3**) and *N*-(aminoalkyl)arylpiperazines (**XII–XVI**). Compound **1** was obtained from 8-bromotheophylline according to described earlier method²⁹. Compounds **2** and **3** were obtained from 8-bromotheophylline in reaction of alkylation with α -chloro ketones in biphasic system, in the presence of potassium carbonate in acetonitrile. *N*-(aminoalkyl)arylpiperazines (**XII–XVI**) were obtained in two steps, according to the Gabriel method⁴⁵, with minor modifications. First, 1-(2-fluorophenyl)- or 1-(3-trifluoromethyl)-phenyl)piperazine (**I–II**) were alkylated in biphasic system, using catalytic amount of potassium iodide with appropriate 2-(bromoalkyl)-1*H*-isoindoline-1,3(2*H*)-dione (**III–V**), in the presence of potassium carbonate in acetonitrile, to give the corresponding phthalimido derivatives. All intermediates were purified by column chromatography using dichloromethane/methanol (9/1) as an eluent. Next, phthalimido derivatives were hydrolyzed with hydrazine monohydrate to afford the *N*-(aminoalkyl)arylpiperazines (**XII–XVI**)⁴⁵. Final ligands

4–21 (Scheme 1) were synthesized as a result of cyclocondensation of 7-ketonyl derivatives of 8-bromotheophylline (**1–3**) with corresponding *N*-(aminoalkyl)arylpiperazines (**XII–XVI**), occurs by refluxing the in 2-methoxyethanol (Scheme 1). Note, in this condition, final compounds were obtained in good to moderate yields, depending on 7-ketonyl derivatives of 8-bromotheophylline used. All final compounds **4–21** in order to obtain analytic samples and further biological evaluation, were purified by column chromatography using a mixture of dichloromethane and methanol in various proportion as an eluent. The chemical structure of compounds **4–21** was verified by ¹H, ¹³C and ¹⁹F NMR tests.

Biological evaluation

In vitro examination of the newly synthesized compounds occurred in three steps. First, all of the compounds were tested in assays against cloned 5-HT_{1A} and 5-HT₇ receptors with standard competitive displacement assays and the inhibition constants *K*_i were determined. For structure–activity relationship studies, we examined the impact of three chemical elements: substitution at phenyl ring of LCAPs, the length of the linker between the purine core and LCAPs and substitution at the 7-position of the purine core.

All tested compounds possessed high affinity at 5-HT_{1A}Rs with some binding in the same range as serotonin (*K*_i from 0.1 to 33 nM) (Table 1), but the 3-CF₃-phenyl-piperazinylalkyl derivatives of 1*H*-imidazo[2,1-*f*]purine-2,4(3*H*,8*H*)-diones were more active than their analogs with a 2-F moiety. For example, compound **7** exhibited the lowest affinity (*K*_i = 33 nM), and the affinity of compound **13** was more than six times higher than that of compound **4**. The tetramethylene spacer (C4) between the purine core and LCAPs proved to be optimal for 5-HT_{1A} sites and compounds with the highest affinity (one exception comp. **11**)

belong to this group. This optimal length of spacer leads to an absence of influence of the substituent at 7 position of the purine core for 5-HT_{1A} affinities. In a group of 2-F analogs, it is easier to prove the unfavorable impact of the propyl (C3) alkyl chain than C4 preference. Moreover, the weaker influence of the 2-F substituent on 5-HT_{1A}R affinity exposes the impact of a methyl moiety at the 7-position of imidazo[2,1-*f*]purine-2,4-dione (**5** vs. **8**, **8** vs. **11**, **6** vs. **9**, and **9** vs. **12**). A spectrum of activities was observed for 5-HT₇R, and tested compounds exhibited either a lack of affinity (**4**, **5**, **13**, **16**), or high (comp. **12** *K*_i = 9 nM, comp. **21** *K*_i = 1 nM, comp. **18** and **20** *K*_i = 10 nM) or moderate affinity (comp. **6–11**, **14**, **17**, *K*_i from 20–152 nM) (Table 1). The structure–activity relationship revealed that, in the case of this receptor, 3-CF₃ derivatives in general bound with the highest affinity, and compound **21** with *K*_i = 1 nM belongs to this group. Due to the structural similarity between 5-HT_{1A} and 5-HT₇ receptors, many of the LCAPs described in the literature as 5-HT₇R ligands derive from a structural modification of the terminal fragment present in 5-HT_{1A}R ligands. Moreover, studies have revealed the critical role of the arylpiperazine substitution pattern in determining the receptor affinity. Volk et al.⁴⁶ found out that electron-donating substituents (–OCH₃) were superior to electron-withdrawing (–Cl, –F) for binding to the 5-HT_{1A} and 5-HT₇ receptors. Our study confirmed that 2-F and 3-CF₃ substituents at the phenyl ring of arylpiperazine were highly preferential for the 5-HT_{1A}R over the 5-HT₇R. The influence of substituents 2-F and 3-CF₃ on 5-HT₇ receptor affinity in the group of tested compounds appears to be equivocal, and a spectrum of activities was observed. It appears that, for LCAPs with a terminal fragment based on imidazo[2,1-*f*]purine-2,4-dione, the length of the aliphatic spacer (C5) is decisive for 5-HT₇R affinity. This is in accordance with Leopoldo et al.⁴⁷, who found that, in a group of *N*-(1,2,3,4-tetrahydronaphthalen-1-yl)-4-arylpiperazinealkylamide derivatives,

Table 1. The binding data and cLog *p* of compounds **4–21**.

4-21

Compound	R	n	R ¹	<i>K</i> _i [nM]*		S [†]	cLog <i>p</i>
				5-HT _{1A}	5-HT ₇		
4	2-F	3	–H	11.7 ± 0.8	NA	–	5.67
5	2-F	4	–H	0.6 ± 0.2	508 ± 12.5	0.001	5.34
6	2-F	5	–H	4.8 ± 0.5	119.7 ± 7.3	0.04	4.68
7	2-F	3	–CH ₃	33 ± 2.0	152 ± 3.5	0.21	5.14
8	2-F	4	–CH ₃	1.1 ± 0.1	86.5 ± 5.0	0.01	3.81
9	2-F	5	–CH ₃	2.5 ± 0.2	30.8 ± 3.5	0.08	4.06
10	2-F	3	–C ₆ H ₅	4.9 ± 0.5	88 ± 4.7	0.05	5.75
11	2-F	4	–C ₆ H ₅	6.3 ± 0.2	137 ± 4.5	0.04	4.06
12	2-F	5	–C ₆ H ₅	3.0 ± 0.2	9 ± 1.0	0.33	5.39
13	3-CF ₃	3	–H	1.8 ± 0.1	NA	–	4.12
14	3-CF ₃	4	–H	0.2 ± 0.05	136 ± 5.2	0.001	5.75
15	3-CF ₃	5	–H	0.2 ± 0.04	16 ± 1.2	0.125	5.69
16	3-CF ₃	3	–CH ₃	1.1 ± 0.1	NA	–	5.23
17	3-CF ₃	4	–CH ₃	0.2 ± 0.05	20 ± 2.2	0.01	5.99
18	3-CF ₃	5	–CH ₃	0.6 ± 0.04	10 ± 0.5	0.06	5.73
19	3-CF ₃	3	–C ₆ H ₅	0.3 ± 0.03	59.6 ± 4.0	0.005	5.08
20	3-CF ₃	4	–C ₆ H ₅	0.1 ± 0.02	10 ± 0.9	0.01	4.72
21	3-CF ₃	5	–C ₆ H ₅	0.2 ± 0.04	1 ± 0.2	0.2	5.72

*Data expressed as the mean ± SD of two independent experiments in duplicate.

†5-HT_{1A}/5-HT₇ selectivity.

Table 2. Inhibition of PDE (%) of compounds 4–21.

Compound	PDE4B		PDE10A	
	10 ⁻⁵	10 ^{-5.5}	10 ⁻⁵	10 ^{-5.5}
4	2	0	6	1
5	3	0	6	0
6	1	0	5	0
7	3	0	5	0
8	2	0	4	0
9	6	0	2	0
10	7	0	3	0
11	2	0	9	0
12	3	0	6	0
13	5	0	5	0
14	1	0	0	0
15	0	0	0	0
16	1	0	4	0
17	0	0	3	0
18	1	0	1	0
19	3	0	2	0
20	2	0	3	0
21	4	0	3	0
Theophylline	3	8	2	-5
Papaverine	13	–	78	57
Rolipram	84	75	3	8

Data are expressed as the mean of two independent experiments in duplicate, vehicle control (DMSO).

five methylene units separating the amide moiety and the piperazine ring were preferred for the affinity to 5-HT₇R_s.

The second step of the *in vitro* study was the PDE inhibitory activity of targeted compounds using a bioluminescent detection system, based on the activity of PDEs which utilized second messenger cAMP. The AMP produced from the hydrolysis of cAMP was quantified using an AMP detection reagent that converts AMP directly to ATP. The therapeutic effect of theophylline (bronchodilatory, positive inotropic effect on heart, psychostimulant) has not been attributed to any single mechanism of action, but the inhibition of PDE was the most important. In order to identify which of the mechanisms involved in the central nervous system action of the LCAPs with imidazo[2,1-*f*]purine-2,4-dione as terminal fragment, PDE4B and PDE10A inhibitory activity was measured. It is noteworthy that, to assess the relative importance of receptor-dependent and/or receptor-independent mechanisms of action, the same range of concentrations as for receptor affinity were taken as a measure of PDE inhibitory activity (starting from 10⁻⁵ M). The investigated compounds had weak inhibitory potencies for PDE4B and PDE10A only at an initial concentration of 10⁻⁵ M, and no inhibition was detected at lower concentrations (Table 2, Figure 3). Moreover, the inhibitory effect of the tested compounds was compared with theophylline.

On the basis of the binding affinity results, a series of compounds possessing affinity below 3 nM for 5-HT_{1A}R (5, 8, 9, 12–21) and below 50 nM for 5-HT₇ receptors (9, 12, 15, 17, 18, 20, 21) was selected for functional profile characterization. Intrinsic activity studies were performed using *in vitro* measures of receptor activation. No activation of any of the receptors was observed, and the compounds showed antagonist properties, especially the 5-HT_{1A} (5, 9, 12, 14, 15, 17–21) (Figures 4 and 5). In case of 5-HT₇R, there are significant differences between the binding and functional tests results for selected compounds. The reason for such a discrepancy is not clear, but one have to bear in mind, that the binding experiments are reflecting simply the competition at the level of a binding site which do not require intracellular signaling mechanisms (e.g. G-proteins or cAMP), whereas the functional tests require appropriate cellular machinery in addition to 5-HT₇ receptor expression. In other words,

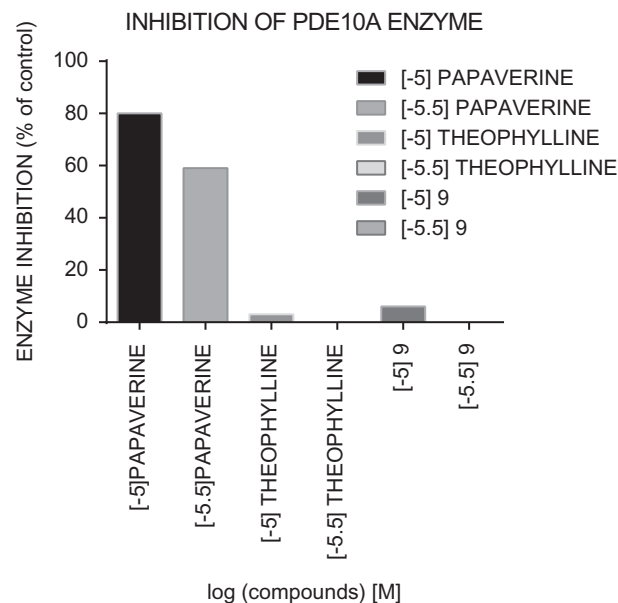


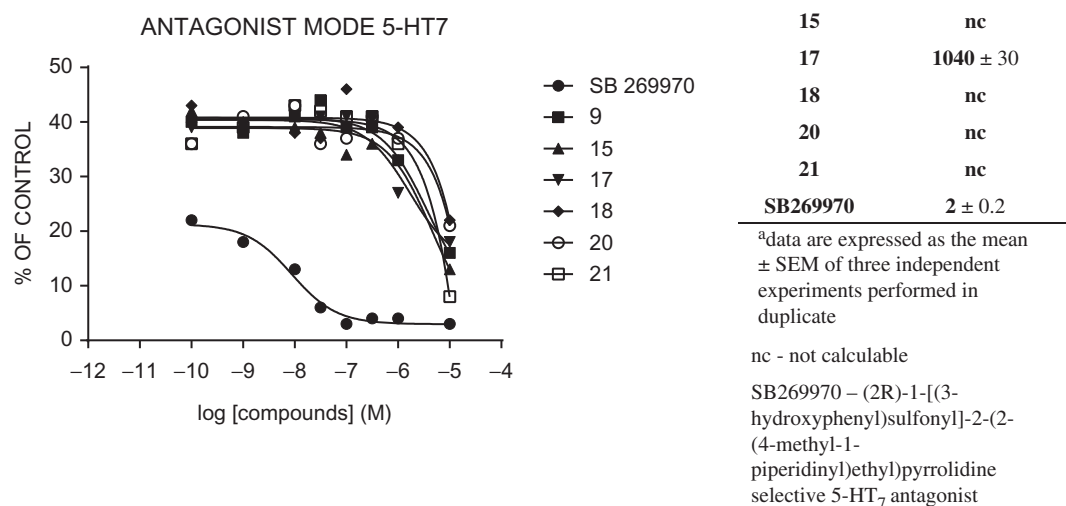
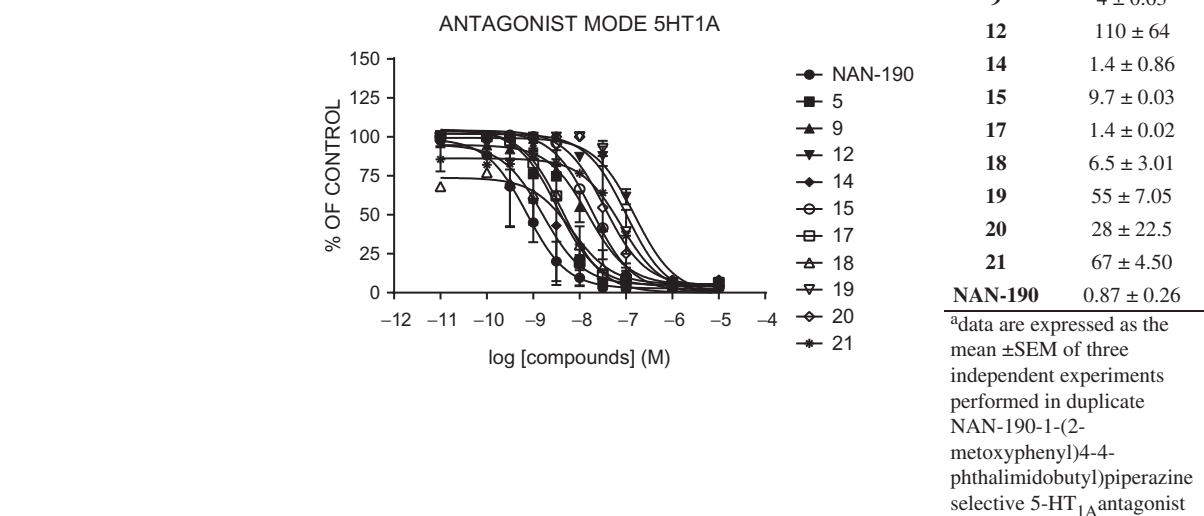
Figure 3. Inhibitor activity (%) against PDE10A for compound 9, theophylline and papaverine in concentration of 10⁻⁵ M and 10^{-5.5} M.

affinity and lack of stimulation of particular signaling pathway is not equal to effective functional antagonism of the receptor. In fact, the functional tests provide additional level of characteristics for the tested compound and are more stringent than binding experiments and therefore constituting good tools to select compounds that are significantly active at 5-HT₇ receptors.

For 5-HT_{1A} receptors, Paluchowska et al.²¹ evaluated a series of 1-substituted 4-(4-arylpiperazin-1-yl)cyclohexane derivatives with different cyclic imide/amide termini, and their flexible tetramethylene analogs. Functional examination revealed that rigid ligands with 2-OCH₃ groups in the aryl moiety and a cyclic imide system in the opposite terminal behaved like 5-HT_{1A} receptor antagonists. On the other hand, unsubstituted, 3-Cl or 3-CF₃ substituted derivatives, as well as those with a cyclic amide group in the terminal fragment, exhibited agonistic or partial agonistic activity. Our study revealed that for LCAPs with terminal fragments based on imidazo[2,1-*f*]purine-2,4-dione and a tetramethylene spacer, ligands with 3-CF₃ group in the aryl moiety (14, 17, 20) showed 5-HT_{1A} antagonist properties. Interestingly, in the group of ligands with a 2-F moiety and tetramethylene spacer, only compound 5 exhibited the ability to inhibit the 5-HT_{1A} receptor. Elongation of the spacer from C4 to C5 for 2-F (9 and 12) and 3-CF₃ (14 vs. 15, 17 vs. 18, 20 vs. 21) derivatives caused decreased in a value of K_b. The above observation indicates that not only the combination of structural features of arylpiperazinealkyl moiety found to be connected with the antagonistic properties of the ligands, but their overall effect also depends on the substitution in 7-position of terminal imidazo[2,1-*f*]purine-2,4-dione fragments.

Lipophilicity

In medicinal chemistry, numerous measured or calculated parameters have been used for the characterization of lipophilicity, but the logarithm of the n-octanol/water partition coefficient (log *p*) is still the generally accepted and primarily applied descriptor of lipophilicity in quantitative structure-activity relationship (QSAR) studies. The lipophilicity of a drug candidate can affect its both pharmacokinetic and pharmacodynamic properties. In particular, the ability of a molecule to cross the cell membrane depends on its partition coefficient³⁶. The MEKC system applied for estimation of lipophilicity uses micelles and closely mimics biological membranes; therefore, it is more

Figure 4. Antagonist mode (K_b) of the selected compounds for 5-HT_{1A} receptor.Figure 5. Antagonist mode (K_b) of selected compounds for the 5-HT₇ receptor.

suitable for physicochemical characterization of bioactive molecules. The “rule of five” defines the range of $\log p$ for good intestinal permeability and penetration to the brain. The estimated $\log p$ values for compounds **6**, **8**, **9**, **11**, **13** and **20** were in ranges defined by the “rule of five” ($\log p < 5$), which indicates good intestinal permeability (Table 1).

Metabolic stability

Metabolic stability is a critical property for drug candidates, because it contributes to oral bioavailability and overall pharmacokinetic performance⁴⁸. Metabolic stability is usually quantified by monitoring the disappearance over time of the parent compound in liver preparations. The disappearance of the parent compound was monitored by calculating the percentage of each compound remaining relative to 0 min and this was plotted

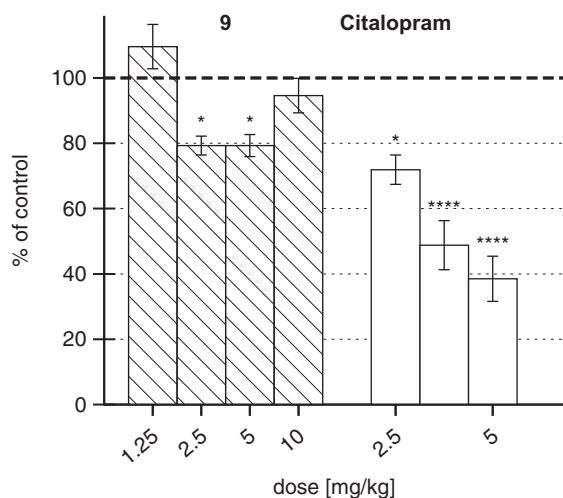
against the incubation time. Currently, commercially available human liver microsomes (HLM) have been the most widely used *in vitro* models for metabolic stability studies⁴⁹. Compounds **9** and **20** were selected for *in vitro* metabolic stability assays. It is noteworthy that this is the first report of the metabolic stability of LCAPs with terminal fragments based on imidazo[2,1-*f*]purine-2,4(3*H*,8*H*-dione). In terms of the conditions of our study, compounds **9** and **20** after 15 min of biotransformation, showed acceptable metabolic stability but **20** was slightly more susceptible to metabolism (Table 3).

Pharmacological *in vivo* evaluation

Finally, compound **9** was selected for further *in vivo* examination on the basis of the following. First, clinical and preclinical studies

Table 3. Metabolic stability screen of compounds **9** and **20** in human liver microsomes (HLM) and major metabolites characteristics.

Comp	[M + H]	Retention time [min]	% of parent comp.	Metabolites				
				ID	[M + H] ⁺	Retention time [min]	% of metabolites	Metabolic pathway
9	482	3.93	43	M1	498	3.35	90	Hydroxylation
				M2	320	3.40	10	Dealkylation
20	580	5.28	39	M1	596	4.33	82	Hydroxylation
				M2	352	4.64	18	Dealkylation



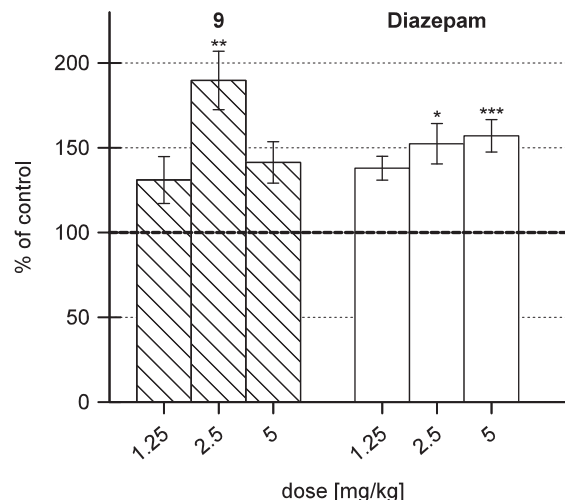
The investigated compound was administered *ip* 60 min, while citalopram 30 min before the test. $n = 6-9$ mice per group.

* $p < 0.05$, **** $p < 0.0001$ vs. vehicle

Figure 6. The effect of the tested compound and 9 citalopram in the forced swim test (FST) in mice.

have shown that antidepressant-like and/or anxiolytic-like effects are mainly produced by serotonin receptor ligands⁵⁰. Compound **9** (8-(5-(4-(2-fluorophenyl)piperazin-1-yl)pentyl)-1,3,7-trimethyl-1*H*-imidazo[2,1-*f*]purine-2,4(3*H*,8*H*)-dione) showed very high 5-HT_{1A} receptor affinity ($K_i = 2.5$ nM) and high 5-HT₇ receptor affinity ($K_i = 30.8$ nM). In our previous studies, a spectrum of receptor activities was observed for compounds with a substituent at the 7th position of the imidazo[2,1-*f*]purine-2,4-dione system. Some compounds were potent 5-HT_{1A} and/or 5-HT₇ receptor ligands with additional affinity for dopamine D₂ receptors. Therefore, to test the feasibility of multireceptor activity, compound **9** was evaluated for affinity for D₂ ($K_i = 437$ nM) and other serotonin subtype (5-HT_{2A,6}, $K_i > 1000$ nM) according to the procedures described earlier^{32,34}. Next, behavioral effects (antidepressant like) similar to those of selective serotonin reuptake inhibitors (SSRIs, e.g. fluoxetine) have been produced by antagonists of 5-HT_{1A} and 5-HT₇ receptors⁵¹. Moreover, an antagonist of 5-HT_{1A} and/or 5-HT₇ receptors induces an anxiolytic-like effect. Compound **9** showed 5-HT_{1A} antagonistic properties exemplified by $K_b = 4$ nM. Our cumulative results prompted us to evaluate the activity of compound **9** in FST and four-plate tests in mice.

Compound **9** (1.25–5 mg/kg), as well as citalopram (1.25–5 mg/kg) used as a reference compound, revealed antidepressant-like properties. Compound **9** administered at two higher doses (2.5 and 5 mg/kg) significantly reduced the immobility time of mice in that test by 21%. The reference antidepressant citalopram shortened (by 28%, 51% and 61%, respectively) the immobility time of mice at all doses (Figure 6). The additional dose (10 mg/kg) of compound **9** have been studied in FST and to check the type



The investigated compound **9** and diazepam were administered *ip* 60 min before the test. $n = 8-10$ mice per group.

* $p < 0.05$, ** $p < 0.01$, *** $p < 0.001$ vs. vehicle

Figure 7. The effect of the tested compound **9** and diazepam in the four-plate test in mice.

of dose–response curve. Compound **9** shows U-shaped dose–response relationship in the forced swim test. Some anxiolytics and antidepressants and newly synthesized compound (**9**) with different mechanisms of action can produce such U-shaped dose–response effects in animal models, for example Millan et al.², Wesolowska et al.⁵².

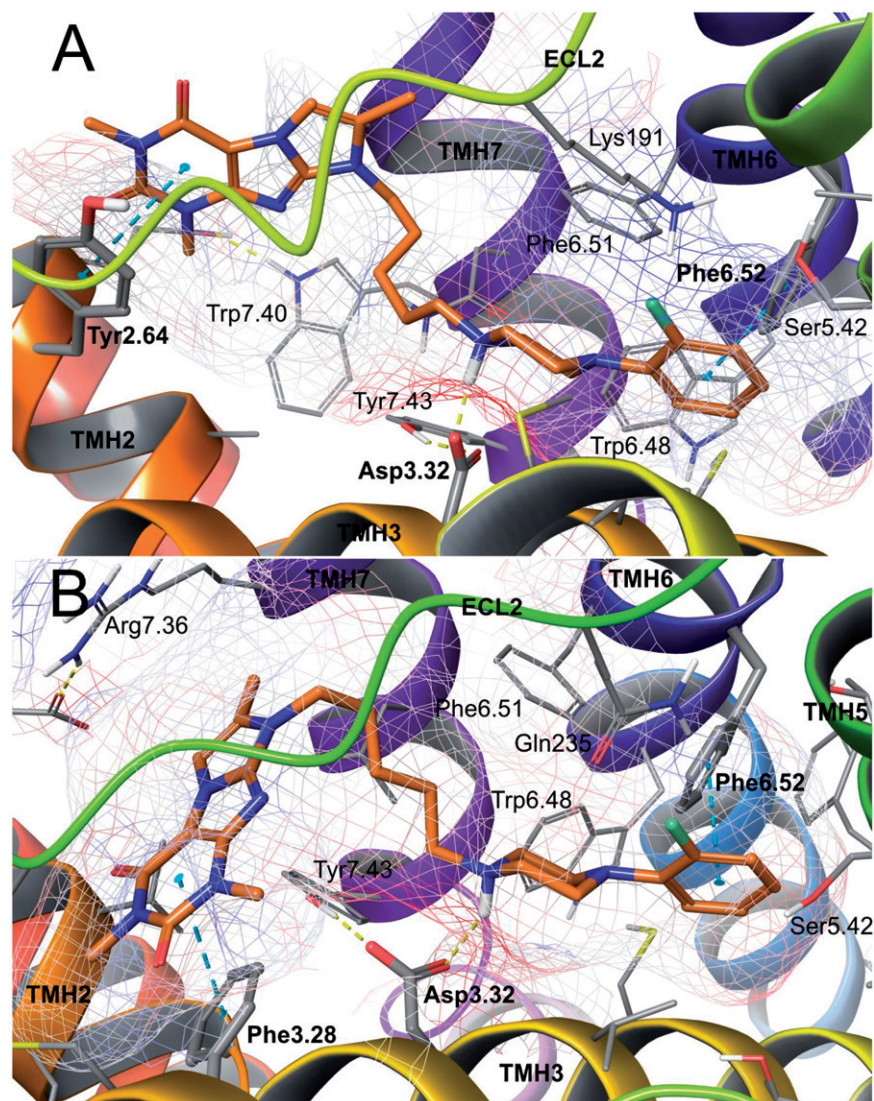
Compound **9** given at a dose of 2.5 mg/kg showed anxiolytic-like activity in the four-plate test, increasing by 90%, in a statistically significant manner, the number of punished crossings accepted by animals during the observation sessions. The reference anxiolytic drug, diazepam, administered at doses of 1.25, 2.5 and 5 mg/kg, significantly increased (by 38%, 52% and 57%, respectively) the number of punished crossings. It is worth noting that the potency of antianxiety effects evoked by **9** (2.5 mg/kg) is greater than that of the reference anxiolytic drug, diazepam, given at the same dose of 2.5 mg/kg. Compound **9** shows inverted U-shaped dose–response relationship in four-plate test. The effects of compound **9** and diazepam in the four-plate test are shown in Figure 7.

Moreover, the antidepressant-and/or anxiolytic-like properties of the investigated agents, citalopram and diazepam, seem to be specific, since when administered at effective doses they did not stimulate spontaneous locomotor activity in mice during the 4 min and 1 min 15 s sessions (i.e. at a time identical to the observation period in the FST and four-plate test, respectively) (data not shown).

Molecular modeling

Docking experiments were performed for compound **9**. The molecule was situated across the two cavities of the binding

Figure 8. Binding modes of compound **9** in the site of 5-HT_{1A} (A) and 5-HT₇ (B) receptors. Amino acid residues engaged in ligand binding (within 4 Å from the ligand atoms) are displayed as sticks, whereas those forming H-bonds (dotted yellow lines) or π - π /CH- π stacking (dotted cyan lines) are represented as thick sticks. Van der Waals molecular surface of the receptor binding site is shown as grid, colored due to electrostatic potential. For the sake of clarity, ECL2 residues were hidden. TMH – transmembrane helix; ECL – extracellular loop.



site: the first one constituted by the transmembrane helices (TMHs) 3–6 in both the receptor models, and the second one between TMHs 2 and 7 (5-HT_{1A} receptor) or TMHs 3 and 7 (5-HT₇ receptor). The anchoring interaction in both sites was a charge-reinforced hydrogen bond between the protonated nitrogen atom of the ligand and the carboxyl group of Asp3.32, as well as the CH- π interactions of the arylpiperazine and aromatic amino acid cluster in the deeper cavity, mainly Phe6.52 (Figure 8). In the case of the 5-HT_{1A} receptor, the electronegative 2-F group of the phenylpiperazine fragment was turned toward the electropositive receptor surface (blue color of the electrostatic potential grid), finding beneficial fluorine-bonding interaction with the side chain residues of Lys191 (the ϵ -amino group) from the second extracellular loop (ECL 2) (Figure 8A). The 5-HT₇ receptor-binding site accepted the 2-fluorophenyl moiety in an analogous manner, exposing an electropositive surface of Gln235 (Figure 8B). The weak fluorine bonding interactions are considered to enrich the ligand–receptor contacts and therefore favorably adjust the ligand binding specificity. The imidazo[2,1-*f*]purine fragment of the molecule occupied the second cavity and established favorable, characteristic for each receptor type, aromatic interactions there. In the 5-HT_{1A} receptor, it interacted by π - π stacking with phenyl ring of Tyr2.64 (Figure 8A). In the 5-HT₇ receptor-binding site, the heterocyclic system formed essential π - π stacking with Phe3.28 (Figure 8B).

Conclusion

In conclusion, the paper presents the synthesis of arylpiperazinyllalkyl derivatives of 1*H*-imidazo[2,1-*f*]purine-2,4(3*H*,8*H*)-dione with 2-fluoro and 3-trifluoromethyl moieties. The study allowed us to identify some potent 5-HT_{1A} (**5**, **14**, **17–21**), 5-HT₇ (**17**, **18**, **20**) and mixed 5-HT_{1A}/5-HT₇ (**12**, **15**, **21**) receptor ligands with weak inhibitory potencies for PDE4B and PDE10A. The study reveals that 5-HT_{1A} and 5-HT₇ receptor affinity benefits from the introduction of a fluorine moiety while introduction of imidazole ring into 7, 8 position of theophylline had no significant effect on inhibitory potencies for selected PDE. The tested compounds were in the ranges defined by the “rule of five” ($\log p < 5$), which indicates good intestinal permeability and showed good metabolic stability. In preliminary pharmacological *in vivo* studies, selected 8-(5-(4-(2-fluorophenyl)piperazin-1-yl)pentyl)-1,3,7-trimethyl-1*H*-imidazo[2,1-*f*]purine-2,4(3*H*,8*H*)-dione (**9**) in the FST in mice behaved as a potential antidepressant. Moreover, potency of anxiolytic effects evoked by **9** in the four-plate test (2.5 mg/kg) is greater than that of the reference anxiolytic drug, diazepam. The binding mode in the 5-HT_{1A} and 5-HT₇ receptors has been elucidated for the representative molecule by means of molecular docking, pointing out favorable interactions, characteristic for each receptor type. Studies might be beneficial to further investigation of the mechanism of CNS action of imidazo[2,1-*f*]purine-2,4(3*H*,8*H*)-dione derivatives.

Declaration of interest

This study was financially supported by the National Science Center Poland (NSC) funded grant based on the decision DEC-2012/07/B/NZ7/01173 and Funds of Statutory Activity UJ CM (K/ZDS/005533). The authors declare no conflict of interest.

References

- Millan MJ. Serotonin 5-HT_{2C} receptors as a target for the treatment of depressive and anxious states: focus on novel therapeutic strategies. *Therapie* 2005;60:441–60.
- Millan MJ, Brocco MD, ekeyne A. Anxiolytic properties of agomelatine, an antidepressant with melatonergic and serotonergic properties: role of 5-HT_{2C} receptor blockade. *Psychopharmacology (Berl)* 2005;77:448–58.
- Wesołowska A. Potential role of the 5-HT₆ receptor in depression and anxiety: an overview of preclinical data. *Pharmacol Rep* 2010; 62:564–77.
- Hedlund PB. The 5-HT₇ receptor and disorders of the nervous system: an overview. *Psychopharmacology (Berl)* 2009;206:345–54.
- Blier P, Ward NM. Is there a role for 5-HT_{1A} agonists in the treatment of depression? *Biol Psychiatry* 2003;53:193–203.
- Naughton M, Mulrooney JB, Leonard BE. A review of the role of serotonin receptors in psychiatric disorders. *Hum Psychopharmacol* 2000;15:397–415.
- Canale V, Kurczab R, Partyka A et al. Towards novel 5-HT₇ versus 5-HT_{1A} receptor ligands among LCAPs with cyclic amino acid amide fragments: design, synthesis, and antidepressant properties. Part II. *Eur J Med Chem* 2015;92:202–11.
- Canale V, Guzik P, Kurczab R et al. Solid-supported synthesis, molecular modeling, and biological activity of long-chain arylpiperazine derivatives with cyclic amino acid amide fragments as 5-HT₇ and 5-HT_{1A} receptor ligands. *Eur J Med Chem* 2014;78:10–22.
- Medina RA, Vázquez-Villa H, Gómez-Tamayo JC, et al. The extracellular entrance provides selectivity to serotonin 5-HT₇ receptor antagonists with antidepressant-like behavior in vivo. *J Med Chem* 2014;57:6879–84.
- Cagnotto A, Salmona M, Casagni A, et al. Ros R. Targeting dopamine D₃ and serotonin 5-HT_{1A} and 5-HT_{2A} receptors for developing effective antipsychotics: synthesis, biological characterization, and behavioral studies. *J Med Chem* 2014;57:9578–97.
- Kowalski P, Mitka M, Jaśkowska J, et al. New arylpiperazines with flexible versus partly constrained linker as serotonin 5-HT(1A)/5-HT(7) receptor ligands. *Arch Pharm (Weinheim)* 2013;346:339–48.
- Zajdel P, Marciniak K, Maślankiewicz A, et al. Antidepressant and antipsychotic activity of new quinoline- and isoquinolinesulfonamide analogs of arripiprazole targeting serotonin 5-HT_{1A}/5-HT_{2A}/5-HT₇ and dopamine D₂/D₃ receptors. *Eur J Med Chem* 2013;60: 42–50.
- Lacivita E, De Giorgio P, Patarnello D, et al. Towards metabolically stable 5-HT₇ receptor ligands: a study on 1-aryl piperazine derivatives and related isomers. *Exp Brain Res* 2013;230:569–82.
- Zajdel P, Marciniak K, Maślankiewicz A, et al. Quinoline- and isoquinoline-sulfonamide derivatives of LCAP as potent CNS multi-receptor-5-HT_{1A}/5-HT_{2A}/5-HT₇ and D₂/D₃/D₄-agents: the synthesis and pharmacological evaluation. *Bioorg Med Chem* 2012;20: 1545–56.
- Lacivita E, Patarnello D, Stroth N et al. Investigations on the 1-(2-Biphenyl)piperazine motif: identification of new potent and selective ligands for the serotonin₇ (5-HT₇) receptor with agonist or antagonist action in vitro or ex vivo. *J Med Chem* 2012;55: 6375–80.
- Volk B, Gacsályi I, Pallagi K, et al. Optimization of (aryl)piperazinylbutyl)oxindoles exhibiting selective 5-HT₇ receptor antagonist activity. *J Med Chem* 2011;54:6657–69.
- Hussainy RA, Verbeek J, van der Born D, et al. Design, synthesis, radiolabeling, and in vitro and in vivo evaluation of bridgehead iodinated analogues of *N*-{2-[4-(2-methoxyphenyl)piperazin-1-yl]ethyl}-*N*-(pyridin-2-yl)cyclohexanecarboxamide (WAY-100635) as potential SPECT ligands for the 5-HT_{1A} receptor. *J Med Chem* 2011;54:3480–91.
- Alonso D, Vázquez-Villa H, Gamo AM, et al. Development of fluorescent ligands for the human 5-HT_{1A} receptor. *ACS Med Chem Lett* 2010;1:249–53.
- Medina RA, Sallander J, Benhamu B, et al. Synthesis of new serotonin 5-HT₇ receptor ligands. Determinants of 5-HT₇/5-HT_{1A} receptor selectivity. *J Med Chem* 2009;52:2384–92.
- Siracusa MA, Salerno L, Modica MN, et al. Synthesis of new arylpiperazinylalkylthiobenzimidazole, benzothiazole, or benzoxazole derivatives as potent and selective 5-HT_{1A} serotonin receptor ligands. *J Med Chem* 2008;51:4529–38.
- Paluchowska MH, Bugno R, Tatarczyńska E, et al. The influence of modifications in imide fragment structure on 5-HT(1A) and 5-HT(7) receptor affinity and in vivo pharmacological properties of some new 1-(*m*-trifluoromethylphenyl)piperazines. *Bioorg Med Chem* 2007;15:7116–25.
- Lepailleur A, Bureau R, Paillet-Loilier M, et al. Molecular modeling studies focused on 5-HT₇ versus 5-HT_{1A} selectivity. Discovery of novel phenylpyrrole derivatives with high affinity for 5-HT₇ receptors. *J Chem Inf Model* 2005;45:1075–81.
- Vermeulen ES, van Smeden M, Schmidt AW, et al. Novel 5-HT₇ receptor inverse agonists. Synthesis and molecular modeling of arylpiperazine- and 1,2,3,4-tetrahydroisoquinoline-based arylsulfonamides. *J Med Chem* 2004;47:5451–66.
- Perrone R, Berardi F, Colabufo NA, et al. Synthesis and structure-affinity relationships of 1-[omega-(4-aryl-1-piperazinyl)alkyl]-1-aryl ketones as 5-HT(7) receptor ligands. *J Med Chem* 2003;46: 646–9.
- Roth BL, Sheffler DJ, Kroeze WK. Magic shotguns versus magic bullets: selectively non-selective drugs for mood disorders and schizophrenia. *Nat Rev Drug Discov* 2004;3:353–9.
- Berton O, Nestler EJ. New approaches to antidepressant drug discovery: beyond monoamines. *Nat Rev Neurosci* 2006;7: 137–51.
- Maxwell CR, Kanes SJ, Abel T, Siegel SJ. Phosphodiesterase inhibitors: a novel mechanism for receptor-independent antipsychotic medications. *Neuroscience* 2004;129:101–7.
- Kanes SJ, Tokarczyk J, Siegel SJ, et al. Rolipram: a specific phosphodiesterase 4 inhibitor with potential antipsychotic activity. *Neuroscience* 2007;144:239–46.
- Zagórska A, Pawłowski M, Siwek A, et al. Synthesis and pharmacological evaluation of novel tricyclic[2,1-*f*]theophylline derivatives. *Arch Pharm (Weinheim)* 2013;346:832–9.
- Partyka A, Jarosz J, Wasik A, et al. Novel tricyclic[2,1-*f*]theophylline derivatives of LCAP with activity in mouse models of affective disorders. *J Pharm Pharmacol* 2014;66:1755–62.
- Zagórska A, Jurczyk S, Pawłowski M, et al. Synthesis and preliminary pharmacological evaluation of imidazo[2,1-*f*]purine-2,4-dione derivatives. *Eur J Med Chem* 2009;44:4288–96.
- Zagórska A, Kołaczkowski M, Bucki A, et al. Structure-activity relationships and molecular studies of novel arylpiperazinylalkyl purine-2,4-diones and purine-2,4,8-triones with antidepressant and anxiolytic activity. *Eur J Med Chem* 2015; 97:142–54.
- Cheng Y, Prusoff W. Relationship between the inhibition constant (K_i) and the concentration of inhibitor which causes 50 per cent inhibition (I₅₀) of an enzymatic reaction. *Biochem Pharmacol* 1973; 22:3099–108.
- Kołaczkowski M, Marcinkowska M, Bucki A, et al. Novel arylsulfonamide derivatives with 5-HT_{6/5}-HT₇ receptor antagonism targeting behavioral and psychological symptoms of dementia. *J Med Chem* 2014;57:4543–57.
- Bajda M, Gula A, Więckowski K, Malawska B. Determination of lipophilicity of γ -butyrolactone derivatives with anticonvulsant and analgetic activity using micellar electrokinetic chromatography. *Electrophoresis* 2013;34:3079–85.
- Waring MJ. Lipophilicity in drug discovery. *Expert Opin Drug Discov* 2010;5:235–48.
- Porsolt RD, Bertin A, Blavet N, et al. Immobility induced by forced swimming in rats: effects of agents which modify central catecholamine and serotonin activity. *Eur J Pharmacol* 1979;57: 201–10.
- Aron C, Simon P, Larousse C, Boissier JR. Evaluation of a rapid technique for detecting minor tranquilizers. *Neuropharmacology* 1971;10:459–69.
- Kołaczkowski M, Bucki A, Feder M, Pawłowski M. Ligand-optimized homology models of D₁ and D₂ dopamine receptors: application for virtual screening. *J Chem Inf Model* 2013;53: 638–48.

40. Kowalski P, Jaśkowska J, Bojarski AJ, et al. Evaluation of 1-arylpiperazine derivative of hydroxybenzamides as 5-HT_{1A} and 5-HT₇ serotonin receptor ligands: an experimental and molecular modeling approach. *J Heterocycl Chem* 2011;48:192–8.
41. Chłoń-Rzepa G, Bucki A, Kołaczkowski M, et al. Arylpiperazinylalkyl derivatives of 8-amino-1,3-dimethylpurine-2,6-dione as novel multitarget 5-HT/D receptor agents with potential antipsychotic activity. *J Enzyme Inhib Med Chem* 2015;25:1–15.
42. Kurowski MA, Bujnicki JM. Genesilico protein structure prediction meta-server. *Nucleic Acids Res* 2003;31:3305–7.
43. Schwede T, Kopp J, Guex N, Peitsch MC. SWISS-MODEL: an automated protein homology-modeling server. *Nucleic Acids Res* 2003;31:3381–5.
44. Sherman W, Day T, Jacobson MP, et al. Novel procedure for modeling ligand/receptor induced fit effects. *J Med Chem* 2006;49:534–53.
45. Gabriel S. Ueber eine Darstellungsweise primärer amine aus den entsprechenden Halogenverbindungen. *Chem Ber* 1887;20:2224–36.
46. Volk B, Barkoczy J, Hegedus E, et al. Phenylpiperazinyl-butyl)oxindoles as selective 5-HT₇ receptor antagonists. *J Med Chem* 2008;51:2522–32.
47. Leopoldo M, Lacivita E, Contino M, et al. Structure-activity relationship study on N-(1,2,3,4-tetrahydronaphthalen-1-yl)-4-aryl-1-piperazinehexanamides, a class of 5-HT₇ receptor agents. 2. *J Med Chem* 2007;50:4214–21.
48. Di L, Kerns EH, Hong Y, et al. Optimization of a higher throughput microsomal stability screening assay for profiling drug discovery candidates. *J Biomol Screen* 2003;8:453–62.
49. Huang J, Si L, Fan Z, et al. In vitro metabolic stability and metabolite profiling of TJ0711 hydrochloride, a newly developed vasodilatory β -blocker, using a liquid chromatography-tandem mass spectrometry method. *J Chromatogr B Analyt Technol Biomed Life Sci* 2011;879:3386–92.
50. Carr GV, Lucki I. The role of serotonin receptor subtypes in treating depression: a review of animal studies. *Psychopharmacology (Berl.)* 2011;213:265–87.
51. Hitchcock SA, Pennington LD. Structure-brain exposure relationships. *J Med Chem* 2006;49:7559–83.
52. Wesołowska A, Nikiforuk A, Stachowicz K, Tatarczyńska E. Effect of the selective 5-HT₇ receptor antagonist SB 269970 in animal models of anxiety and depression. *Neuropharmacology* 2006;51:578–86.

Supplementary material available online